Coordination Chemistry Reviews, 96 (1989) 1–48
Elsevier Science Publishers B.V., Amsterdam – Printed in The Netherlands

NMR STUDIES OF THE DYNAMIC STEREOCHEMISTRY OF SULPHUR AND SELENIUM COMPLEXES OF PLATINUM

KEITH G. ORRELL

Department of Chemistry, The University, Exeter, Devon EX4 4QD (U.K.)

(Received 1 December 1988)

CONTENTS

A. Introduction 1
B. NMR spectroscopy 2
(i) Static NMR parameters 2
(ii) Dynamic NMR time scales 5
(iii) One-dimensional DNMR spectroscopy 7
(iv) Two-dimensional DNMR spectroscopy 8
C. Dynamic structures 10
(i) Platinum(II) complexes 10
(a) Monodentate ligands 10
(b) Bidentate ligands 15
(ii) Platinum(IV) complexes 21
(a) Monodentate ligands 21
(b) Bidentate chelate ligands 22
(c) Bidentate bridging ligands 34
(d) Tridentate ligands 40
(iii) Platinum cluster compounds 42
References 45

A. INTRODUCTION

The high configurational stability of sulphur in species such as sulphonium ions and sulphoxides is well established. However, when sulphur or other group 6 atoms are coordinated to transition metals with *d* orbitals available for π backbonding, then the pyramidal inversion rates of these atoms are greatly enhanced, leading in the case of the chalcogens, sulphur, selenium and tellurium, to configurationally non-rigid species.

The first recognition of a stereochemically non-rigid sulphur ligand complex was in 1966 when the coordinated sulphur atoms in $[PtCl_2(MeSCH_2CH_2SMe)]$ were shown [1] to undergo pyramidal inversion at a rate within the NMR time scale of detection. This work subsequently led to the discovery of widespread fluxionality in sulphur and selenium complexes

0010-8545/89/$16.80

of transition metals. This review describes recent studies of the dynamic stereochemistry of sulphur and selenium ligand complexes of one such transition metal, platinum, in its +2 and +4 oxidation states. Most of the studies have relied heavily on the latest one- and two-dimensional techniques of NMR spectroscopy, and therefore before the literature is reviewed, the pertinent features of these NMR methods will be described.

The literature coverage of the review is for the 5 year period 1983–1987 inclusive.

B. NMR SPECTROSCOPY

It can be convincingly claimed that NMR spectroscopy is now the single most powerful spectroscopic method for investigating molecular structures in the solution phase. Such a claim can be exemplified by the uses made of NMR in the context of this review. In cases where single-crystal X-ray diffraction studies cannot be carried out, NMR is invariably chosen as the alternative structural probe on the strength of its powerful single-pulse and multipulse experiments which now have multinuclear diversity. While these are more usually performed on liquid phase samples, such a restriction is rapidly diminishing with the increasing versatility of high resolution NMR applied to polycrystalline solids.

(i) Static NMR parameters

The NMR nuclei which are most clearly relevant to the title complexes of this review are the common spin-1/2 nuclei ^{1}H and ^{13}C and the less-common nuclei ^{33}S ($I = 3/2$), ^{77}Se ($I = 1/2$) and ^{195}Pt ($I = 1/2$). ^{1}H and ^{13}C are the preferred nuclei in the vast majority of cases, but the limited chemical shift dispersion of ^{1}H and the low receptivity of ^{13}C at times demand recourse to the other nuclei listed above, particularly ^{195}Pt.

The isotope ^{33}S is a quadrupolar nucleus ($I = 3/2$) with a natural abundance of 0.76% and a receptivity, relative to protons, of 1.71×10^{-5}. While this receptivity is a factor of only 10 below that of ^{13}C, the electric quadrupole moment of ^{33}S (-6.4×10^{-34} m^2) can lead to extensive line broadening by virtue of rapid spin–spin relaxation. While ^{33}C chemical shifts can occur over a range of 800–1000 ppm [2,3], linewidths can vary considerably and somewhat unpredictably, and despite recent efforts [4] to overcome basic experimental difficulties in recording good quality ^{33}S spectra, published ^{33}S data are still limited to relatively common, low molar mass compounds [5], and, it would seem, no ^{33}S NMR spectra have been reported of sulphur ligands coordinated to transition metals.

^{77}Se ($I = 1/2$) with a natural abundance of 7.58% and receptivities of

5.26×10^{-4} (relative to ^{1}H) and 2.98 (relative to ^{13}C) is routinely studied with modern Fourier transform (FT) NMR spectrometers [3]. With its chemical shifts ranging over about 2000 ppm, the nucleus can be used as a sensitive probe of chemical environment, and it has been extensively exploited in organoselenium chemistry [6] and selenium coordination chemistry [7]. ^{77}Se NMR spectra are usually recorded under proton noise decoupling conditions, the maximum possible $^{77}Se-\{^{1}H\}$ nuclear Overhauser enhancement, η, being 2.62. However, the dipole–dipole mechanism of ^{77}Se relaxation is often of minor importance, in contrast with ^{33}S relaxation, and the dominant mechanisms are usually chemical shielding anisotropy (CSA) and spin rotation (SR) [8]. One-bond coupling constants involving selenium and other spin-1/2 nuclei are usually measured with ease, the typical range of values for Pt–Se ligand complexes being 700 to about −100 Hz. For Pt(IV)–Se complexes, $^{1}J(^{195}Pt,^{77}Se)$ values fall in the range 340–200 Hz [9].

^{195}Pt is one of the most suitable and informative of all transition metal nuclides for NMR study. This stems from its very favourable nuclear properties, i.e. $I = 1/2$, natural abundance of 33.7%, a relatively large magnetic moment, $\mu/\mu_N = 1.0398$, and a receptivity of 3.36×10^{-3} relative to protons, which is 19 times higher than that of ^{13}C. These factors, coupled with the very favourable spin–lattice and spin–spin relaxation times, have caused a rapid growth in ^{195}Pt NMR studies [10]. Most ^{195}Pt T_1 values are shorter than 2 s as a result of efficient relaxation via CSA and SR mechanisms. The different temperature dependences of these contributions are important in the context of variable-temperature dynamic NMR (DNMR) (see later). On decreasing the temperature, whereas T_1(SR) values increase in magnitude, T_1(CSA) values decrease and this can have misleading consequences in certain circumstances. For instance, protons coupled to platinum may not show ^{195}Pt satellites at low temperatures owing to very short T_1(CSA) values, which produce broadening of the satellites to an extent that they may not be distinguished from the main proton signals [10]. Therefore the absence of ^{195}Pt satellites in low temperature proton spectra should not necessarily be interpreted as due to lack of Pt–ligand coordination. In our experience, this feature is associated more with platinum(II) complexes than with platinum(IV) complexes.

The magnetic field dependence of the CSA contribution can also have a similar negative influence of ^{195}Pt spectra. For example, at very high fields the satellite linewidths can be adversely affected, and the signals difficult to detect. For practical purposes an operating field of around 6 T (equivalent to a ^{1}H resonance frequency of about 250 MHz) is sufficiently large for all ^{195}Pt studies, given the normally large chemical dispersion exhibited by this isotope.

^{195}Pt chemical shifts have been detected over a range of about 15 000

ppm, and thus the likelihood of ^{195}Pt signal overlap is diminishingly small. Shifts are dominated by changes in the paramagnetic screening contribution of the Ramsay equation which involves, amongst other terms, the inverse cube of the valence *d*-electron radius $\langle r^{-3} \rangle_{5d}$. This term is the primary cause of the very large chemical shift range of ^{195}Pt [10]. Variations within this range are particularly an inverse function of ΔE, the difference between the energies of unoccupied and occupied molecular orbitals in the complex being studied. Knowledge of this parameter is nearly always imprecise and thus resort is usually made to empirical parameterized expressions [11]. In a recent review [12], Mason has attempted to rationalize shifts of ^{195}Pt, amongst other transition metal nuclides, to spectrochemical and nephelauxetic effects of the ligands in metal complexes. Attention was particularly drawn to the complementarity of NMR and optical spectroscopy since both techniques depend on the propensity of the transition metal and ligands to split the ligand field and to expand the *d*-electron shell.

In observational terms, the following generalizations of ^{195}Pt shifts are usually valid.

(i) Substitution of a relatively hard A-type ligand (e.g. H_2O or Cl^-) for a "softer" ligand which coordinates more strongly to platinum(II) (e.g. H^-, CH_3^-, SR_2^-) induces a relatively large high frequency shift (500–1000 ppm or more).

(ii) There is an approximate dependence on oxidation state with platinum(IV) > platinum(II) > platinum(0), but the nature of the ligand can often be as important as the metal oxidation state.

(iii) Shifts vary with the halogen, such that low frequency shifts are associated with increasing atomic number. For example, in the series $[PtXMe_3(MeSeCH_2CH_2SeMe)]$ (X = Cl, Br or I) [9] the shifts (relative to 21.4 MHz) are 1257 (Cl), 1125 (Br) and 935 (I) ppm.

(iv) The shifts are a sensitive function of the complex geometry, e.g. *cis*/*trans* or *meso*/DL distinction.

Referencing of ^{195}Pt shifts is often carried out relative to $PtCl_6^{2-}$, despite the solvent dependence of this anion and its high frequency signal which causes virtually all associated δ values to be negative. An alternative method which avoids these problems is the use of the absolute frequency scale Ξ defined relative to the ^1H signal of Me_4Si at exactly 100 MHz. For platinum, $\Xi(^{195}Pt) = 21.4$ MHz is commonly chosen and will be adopted in this review. This leads to the relationship

$$\delta(PtCl_6^{2-}) = \delta(21.4\ \text{MHz}) - 4533$$

for relating the two frequency scales. ^{195}Pt shifts should always be quoted for a given temperature, since many of the shifts have sizeable temperature coefficients; 1 ppm K^{-1} is not uncommon.

^{195}Pt spin coupling constants are important parameters of chemical structure, and comprehensive collections of $^{1}J(^{195}Pt,^{1}H/^{13}C)$ and $^{2}J(^{195}Pt,^{1}H/^{13}C)$ have been compiled. Platinum is one of the few transition metals where two-, three-, four-, five- and six-coordination is to be found. Generally, coordination numbers 2–5 (usually platinum(0) and platinum(II)) give larger ^{1}J(Pt,L) (L = ligand) values than the related six-coordinate (usually platinum(IV)) complexes. This may be rationalized in terms of the larger percentage *s* character of the metal in its lower oxidation state, which influences the magnitude of the Fermi contact term of the full spin–spin coupling expression. For a given oxidation state, the variation in ^{1}J(Pt,L) or ^{2}J(Pt,L) values depends on such factors as the nature of the *trans* ligand, ligand ring size and ligand geometry. For platinum(IV) complexes of type $[PtXMe_3\{MeE(CH_2)_nE'Me\}]$ (E,E′ = S or Se; X = Cl, Br or I), ^{1}J(Pt,C) values lie in the range 600–700 Hz [9] and ^{2}J(Pt,H) values in the range 69–73 Hz [13].

Magnitudes of ^{n}J(Pt,Pt) couplings are of particular interest in the context of platinum cluster chemistry. It is now fairly clear that ^{n}J(Pt,Pt) values do not correlate well with Pt–Pt bond lengths. Nevertheless, certain ground rules are becoming established. The ^{2}J(Pt,Pt) values lie in the range 125–390 Hz when platinum(II) atoms are bridged by halogen atoms, and in the range 200–970 Hz when bridged by S^{2-} or RS^{-}. When platinum(IV) atoms are bridged by these groups, the *J* values are appreciably smaller, and in the case of binuclear halogen-bridged complexes $[(PtXMe_3)_2L–L']$ (L–L′ = bridging chalcogen ligand) are unobservably small [14]. By contrast, for dimeric complexes with definite Pt–Pt bonds, ^{1}J(Pt,Pt) values can be quite large, being often greater than 3 kHz for platinum(I) or platinum(II) complexes.

High resolution solid state ^{195}Pt NMR is still in its infancy but is likely to be more widely exploited in the near future. No Pt–S or Pt–Se complexes have yet been examined in the solid state but studies on four platinum(IV) complexes and one platinum(II) complex have revealed detailed information on the anisotropy of the ^{195}Pt shielding tensor [15].

(ii) Dynamic NMR time scales

This review is concerned with the dynamic stereochemical features of complexes containing Pt–S or Pt–Se bonds. Studies of stereochemical non-rigidity are invariably performed by NMR spectroscopy and so it is appropriate to highlight the features of this technique which make it uniquely suited to monitoring relatively slow rates of molecular rearrangements.

The response of any spectroscopic method to dynamic processes depends on the response time or interaction time of that technique to the molecular

TABLE 1

NMR time scales of chosen nuclides

Nucleus	Approximate shift range (ppm)	Shift ($\Delta\nu$) at 5.87 T [a] (kHz)	Time scale range τ [b] for 5.87 T shifts	Typical operating time scale τ [c]	Rate constant k [a] (s^{-1})
^{1}H	0–10	0–2.5	0.45 s–180 μs	18 ms	55
^{13}C	0–250	0–62.5	0.45 s–7.2 μs	720 μs	1.4×10^{3}
^{77}Se	0–2000	0–500	0.45 s–0.9 μs	90 μs	1.1×10^{4}
^{195}Pt	0–15000	0–3750	0.45 s–0.12 μs	12 μs	8.3×10^{4}

[a] Corresponds to ^{1}H spectra at 250 MHz. [b] Based on eqn. (1) with $\Delta\nu = \Delta\nu_{max}$ (e.g. 2.5 kHz for ^{1}H) and $\Delta\nu_{min} = 1$ Hz. [c] Based on eqn. (1) with $\Delta\nu = \Delta\nu_{max}/100$. [d] $k = \tau^{-1}$.

movement. This so-called "time scale" is loosely related to the reciprocal of the frequency of electromagnetic radiation utilized by that technique. In that sense, NMR is a "slow" technique (i.e. it is responsive to slow rates of movement) compared with other techniques such as IR or UV–visible spectrophotometry [16]. Whereas the latter techniques always identify mixtures of "static" species, NMR can reveal either static species or time-averaged responses, depending on the rate of the dynamic process. The latter can, of course, be controlled by temperature, and so many NMR spectra can be moved from the slow to the fast exchange regime by sample temperature variation. Computations of the observed bandshape changes can give precise rates and activation energies of the dynamic processes. However, with the plethora of NMR experiments currently available a more precise definition of NMR time scale is clearly needed. This parameter can vary enormously depending on which spectral feature(s), namely, signal intensities, chemical shifts, scalar couplings, or nuclear relaxation times is (are) changed or modulated by the dynamic process [17]. Such processes can be followed either as a function of time for samples under non-equilibrium conditions or as a function of temperature for samples at chemical equilibrium. In time-dependent NMR, signal intensities are monitored, whereas in temperature-dependent NMR it is the chemical shift and scalar couplings which are usually affected. Most NMR applications in this review refer to equilibrium processes and thus the NMR time scale will be defined in that context.

This time scale depends on the chemical shift difference parameters $\Delta\nu_i$ being modulated. The magnitude of $\Delta\nu_i$ depends both on the nucleus being detected and the type of fluxional process being followed. In Table 1 typical dynamic NMR (DNMR) characteristics of the four nuclides most relevant to this review are listed. The time scales, τ, are calculated from the standard formula for band coalescence of two equally intense exchanging signals:

$$\tau = k^{-1} = \sqrt{2}/\pi\Delta\nu \qquad (1)$$

where k is the first-order rate constant for the process and the chemical shift difference values, $\Delta\nu$, are chosen as the maximum shift difference for that nucleus and the minimum resolvable shift difference (taken as 1 Hz). In practice, $\Delta\nu$ values will be a small fraction of the total shift range possible, and so the last column in Table 1 gives the time scales based on $\Delta\nu$ being 1% of $\Delta\nu_{max}$.

The values obtained show that the time scales are in the microsecond range but vary appreciably with the nucleus, such that, compared with the ^{1}H time scale, the ^{13}C scale is 25 times shorter and the ^{195}Pt scale about 10^3 times shorter. This means that, for example, ^{195}Pt spectra are sensitive to rate processes about 10^3 times faster than are ^{1}H spectra, all other factors being unchanged. Thus the fastest (lowest energy) fluxional processes may not be too fast to be followed by low temperature ^{195}Pt spectroscopy, while the slowest (highest energy) processes are most likely to be detected by high temperature ^{1}H spectra. The practical consequences of this are that fluxional processes with activation energies in the approximate range 30–100 kJ mol^{-1} can be detected by standard one-dimensional (1D) NMR bandshape methods based on chemical shift averaging effects.

Such activation energies may be expressed as E_a values using the Arrhenius rate theory or as $\Delta H^{\ddagger}$ and $\Delta G^{\ddagger}$ values using the Eyring theory. The latter approach is preferable since its parameters afford a more precise chemical interpretation than do the Arrhenius parameters. In particular, through the thermodynamic relationship

$$\Delta G^{\ddagger} = \Delta H^{\ddagger} - T\Delta S^{\ddagger} \qquad (2)$$

it is possible to calculate $\Delta G^{\ddagger}$ values for any chosen temperature if $\Delta H^{\ddagger}$ and $\Delta S^{\ddagger}$ are known from variable-temperature bandshape fittings. $\Delta G^{\ddagger}$ values have been shown to be least prone to systematic error and so these values, normally calculated at 298.15 K, are used for comparing energies of fluxional processes.

(iii) One-dimensional DNMR spectroscopy

Total bandshape analysis techniques should be employed whenever possible using standard fitting programs such as DNMR3 [18]. If the spectral complexity is such that this approach cannot be used, an approximate value for $\Delta G^{\ddagger}(T_c)$ may be found from the rate constant evaluated using eqn. (1) at the coalescence temperature(s) (T_c) of the dynamic spectrum. Highest accuracy in bandshape analysis is achieved when spectra of moderate complexity exhibit exchange broadening over a wide temperature range, with the static spectral parameters (i.e. natural linewidths, $(\pi T_2^*)^{-1}$, chemical shifts, and nuclear site populations) showing no temperature variation. Such DNMR

methods have been very widely exploited for all types of intramolecular and intermolecular rearrangements [19]. Recent reviews of these methods have described applications in inorganic and organometallic chemistry [20] and in the chemistry of metal complexes of sulphur, selenium and tellurium ligands [7]. The present review may therefore be regarded as an update to certain aspects of these earlier reviews.

The NMR time scales in Table 1 refer to chemical shift modulation, but there may be instances when a fluxional process is slow on the chemical-shift-based time scale but fast on the nuclear relaxation time scale. Such circumstances allow population information to be transferred from one nuclear site to another; this is the basis of selective transfer techniques [21]. Such techniques have been particularly championed by Mann for organometallic polyene and polyenyl complexes [22]. The great virtue of this approach is that it allows exchange information to be deduced from NMR spectra which are in the "slow" exchange regime and exhibit no exchange broadening. It thus effectively increases the time scale of the technique, in practice by a factor of at least 100, over the chemical-shift-based time scale. The upper limit of the time scale thus becomes about 50 s, which means that rate constants of the order of 0.02 s^{-1} can be measured with accuracy. Instead of saturating certain signals they can be inverted with selective π r.f. pulses. This is the spin population inversion (SPI) technique and it uses the same pulse sequence as that used to produce transient nuclear Overhauser effects (NOEs), namely

$$\pi - \tau_m - \pi/2 - \text{Acquire}$$

By varying the mixing time τ_m between the selective π pulse and the non-selective $\pi/2$ read pulse the resulting intensity variation in the other exchanging signals provides exchange rate information. In non-exchanging systems any signal intensity changes are the result of cross-relaxation NOE effects, and varying τ_m values can provide spatial information about the interacting nuclei.

(iv) Two-dimensional DNMR spectroscopy

There is a powerful two-dimensional (2D) analogue of the above SPI experiment which will now be summarized. It is based on the 2D-NOESY pulse sequence

$$\pi/2 - t_1 - \pi/2 - \tau_m - \pi/2 - \text{Acquire}$$

and involves measuring spectra as a function of different intervals, t_1, between a pair of non-selective $\pi/2$ pulses for a given mixing time τ_m. Double Fourier transformation produces 2D spectra which consist of diago-

nal signals plus off-diagonal signals (cross-peaks) which have built up during the mixing time τ_m. When these cross-peaks are due to chemical exchange rather than cross-relaxation magnetization transfer the spectra are referred to as 2D-EXSY spectra. A comprehensive review of this technique has been presented recently by Willem [23], to which the reader is referred for further details.

One of the major advantages of this approach to stereochemical problems over 1D bandshape or magnetization transfer experiments is its straightforward applicability to multisite exchange problems. Furthermore, it avoids the subjectivity of 1D bandshape fittings or the iterative nature of calculations based on magnetization transfer experiments. It depends instead on a judicious choice of the mixing time, τ_m, and the accuracy of the measuring signal intensities on the 2D spectral map.

One of the first demonstrations of the quantitative accuracy of 2D-EXSY experiments involved the Pt(IV)–(sulphur ligand) complexes [$PtXMe_3$-($MeSCH_2CH_2SMe$)] (X = Cl, I) [24]. Accurate rate constants associated with the pyramidal inversion characteristics of the coordinated sulphur atoms had previously been established by ^1H 1D bandshape analysis [25]. These rate constants were associated with the interconversion of the "static" invertomers shown in Scheme 1.

In order to avoid the possibility of cross-relaxation effects, ^{195}Pt was chosen as the probe nucleus. ^{195}Pt 2D-EXSY spectra were measured over the temperature range 223–282 K and with mixing times in the range 0.015–1.5 s. Conversion of signal intensities to rate constants was achieved by a general computational procedure which did not require any precise knowledge of ^{195}Pt T_1 values. The rate constants so obtained were in excellent accord with the 1D-derived values and showed conclusively that the sulphur atom pairs inverted independently. The smallest 1D-derived rate constants

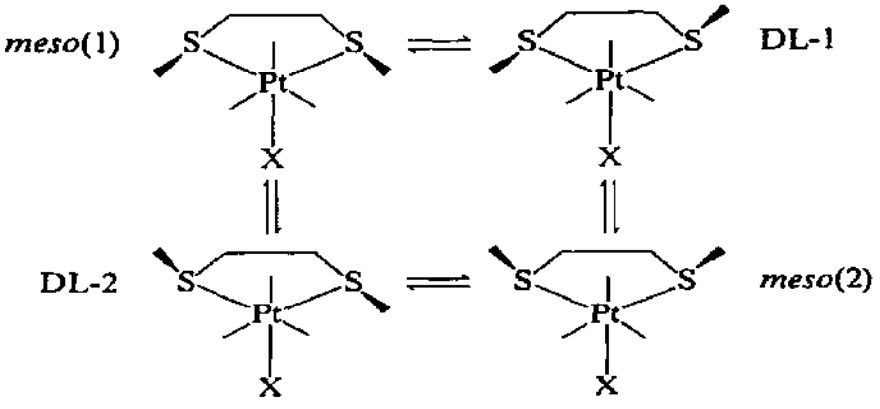

Scheme 1.

were about 1 s^{-1} whereas 2D-EXSY values could be reliably measured down to 0.0094 s^{-1} for a temperature 50 °C below the lowest usable 1D spectral temperature.

It is important to be aware of the fact that weaker second-order cross-peaks can appear in 2D-EXSY spectra if the chosen mixing time is longer than the optimal value. This does not affect the subsequent calculation of exchange rates using the D2DNMR method [24] but it does offer a warning that the presence of cross-peaks does not necessarily indicate direct exchange between the species involved. Molecular exchange mechanisms based only on qualitative interpretations of 2D-EXSY contour maps are therefore subject to uncertainties.

C. DYNAMIC STRUCTURES

This section of the review will discuss the stereodynamics of platinum(II) and platinum(IV) complexes with coordinated sulphur or selenium ligands. The literature appears to be restricted to these two oxidation states of platinum. Earlier studies of these two classes of complexes by DNMR methods have featured in parts of existing reviews [7,20].

(i) Platinum(II) complexes

(a) Monodentate ligands

Platinum(II) *trans*-dihalide complexes of cyclic sulphides have been known

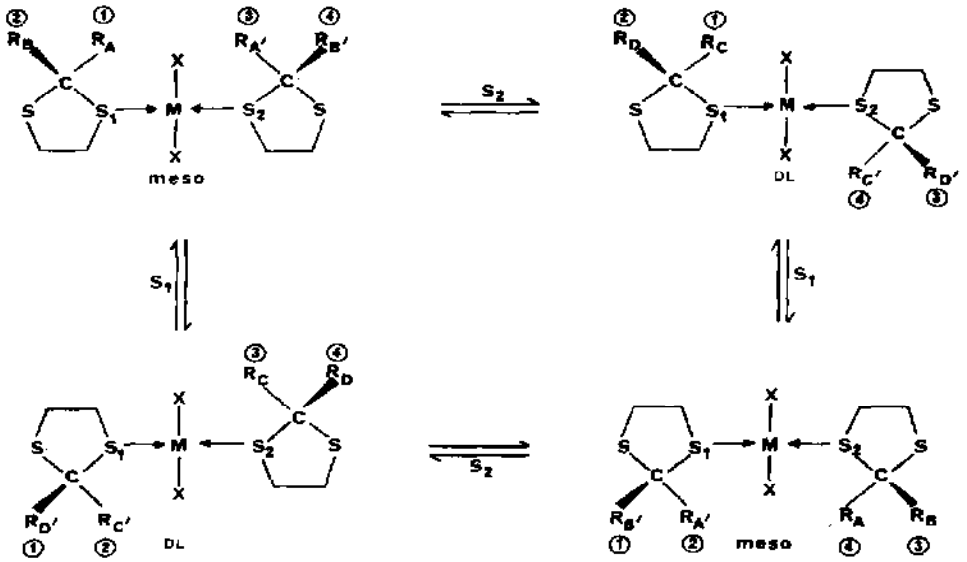

Scheme 2.

for a considerable time [26] and some of them have been extensively studied by DNMR in order to characterize the pyramidal inversion of the coordinated sulphur atoms [27]. More recent studies [28] have been directed towards analogous 1,3-dithiolane complexes $[PtCl_2(\overline{SC_2H_4SCR_2})_2]$ (R = H, Me) in order to assess the influence of a second heterocyclic sulphur atom on the inversion rate of the platinum-coordinated sulphur atom, and to establish whether the platinum atom underwent a 1,3-shift between the two sulphur sites since such shifts were known to occur in metal complexes of open-chain ligands such as $MeSCH_2SMe$ [29] and cyclic ligands such as $\overline{SCH_2SCH_2SCH_2}$ [30].

The ^1H and ^{13}C NMR spectra of the *trans* complexes recorded at low temperatures gave evidence of two equally abundant solution species. These were recognized as the *meso* and DL forms of the complex, which could be interconverted by pyramidal inversion of either sulphur atom (Scheme 2). This dynamic process was measured by the exchange of the protons (or methyl groups) of the isolated carbon atom. The dynamic ^1H spin system is

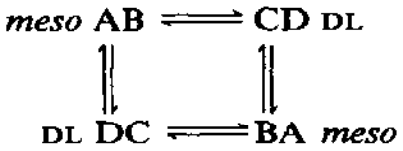

if the ^{195}Pt satellites are ignored. Bandshape fittings of the variable-temperature ^1H spectra yielded $\Delta G^{\ddagger}$ values of 63.9 ± 0.2 (R = H) and 56.0 ± 0.1 kJ mol^{-1} (R = Me). In the case of $[PtCl_2(\overline{SC_2H_4SCH_2})_2]$ it was notable that the $-SC_2H_4S-$ proton signals collapse to a singlet simultaneously with the $-SCH_2S-$ signal. This suggests the occurrence of a 1,3-Pt–S shift correlated with the sulphur inversion process. By contrast, the 2,2-dimethyldithiolane complex shows no such 1,3-metal shift, implying that the bulky $-CMe_2-$ group between the two sulphur atoms prevents easy access to the transition state associated with the 1,3-Pt–S commutation. The precise mechanism of this concerted sulphur inversion and 1,3-shift fluxion is not known, but a dissociation–recombination process can be discounted since separate free and coordinated ligand signals were observed after the onset of pyramidal inversion.

Related studies [28] on the monosubstituted 1,3-dithiolane complexes $[PtCl_2(\overline{SC_2H_4SCHR})_2]$ (R = Me, ^{t}Bu, Ph) showed no evidence of any sulphur inversion or 1,3-Pt-shift fluxionality up to about 60 °C. In solution these complexes exist solely as the *meso* (R, *trans / trans*) (**1**) and DL (R, *trans / trans*) (**2**) species. These isomers belong to different invertomer sets

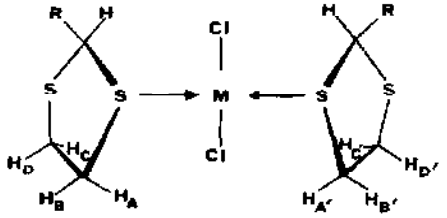

1

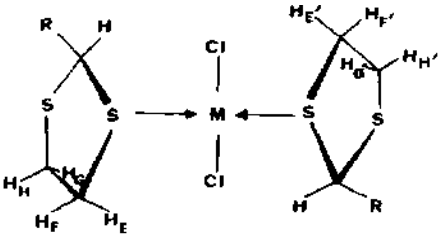

2

which cannot be interconverted simply by sulphur inversion. The other invertomers were not detected since they all involve one of the R groups in a sterically crowded environment. The related palladium(II) complexes showed evidence of 1,3-metal shifts coupled with ligand dissociation–recombination, unlike the platinum(II) complexes.

Dimethyl sulphoxide (DMSO) is an ambidentate ligand, as illustrated by the complex $[Pt(DMSO)_4]^{2+}$ which contains two *cis* O-bonded DMSO ligands and two *trans* S-bonded ligands. Oxygen-bound DMSO species tend to undergo more rapid substitution than S-bound species. Rates of S-bonded DMSO replacement can be followed conveniently by time-dependent NMR methods, and there have been a number of recent studies of this type involving platinum(II) complexes.

One of these described the kinetics and mechanisms of ligand exchange, substitution and isomerization of DMSO–amino acid complexes of platinum(II) [31]. Substitution of Cl^- by DMSO in the complexes [Pt(amino acid)Cl_2] (amino acid = glycine, sarcosine, *N*,*N*-dimethylglycine and proline) afforded *cis*(N,S)- and *trans*(N,S)-[Pt(amino acid)(DMSO)Cl] complexes (**3** and **4**). The reversible isomerization of these isomers was also

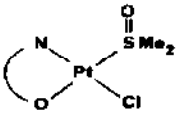

3

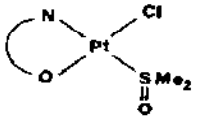

4

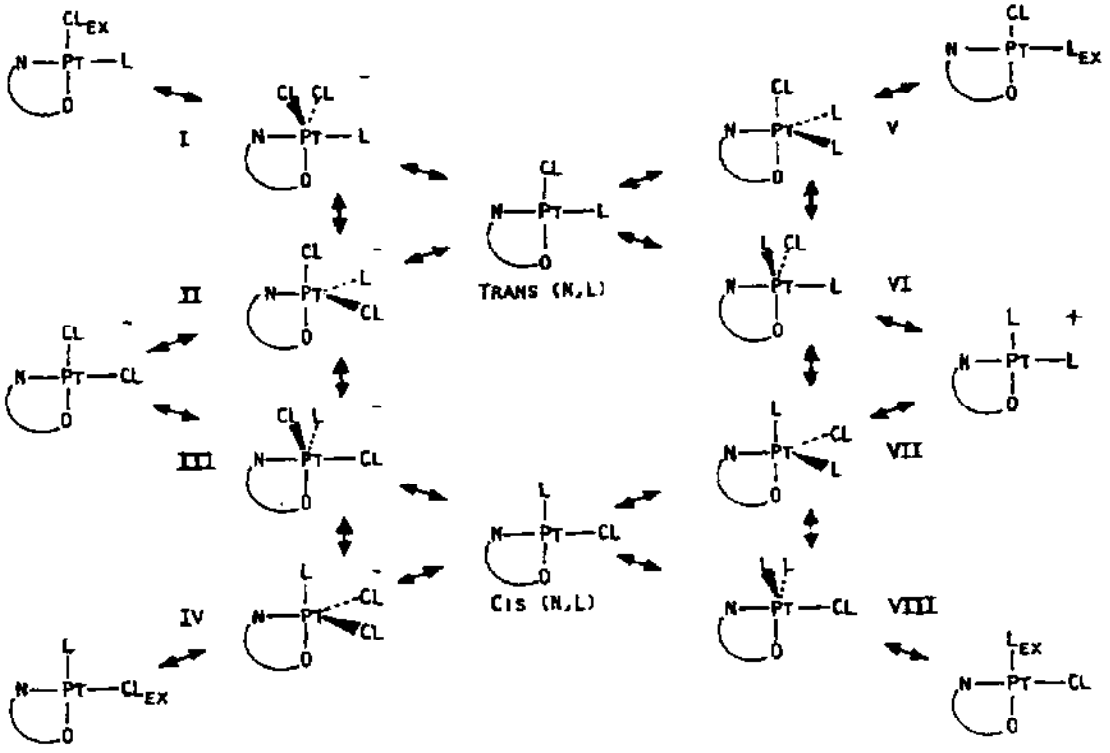

Scheme 3.

studied. Rate data derived from NMR and radioisotope techniques show that a pseudorotation (turnstile) mechanism for DMSO-catalysed isomerization predominates by a factor of 4–20 over a consecutive displacement mechanism for Cl^--catalysed isomerization. A general mechanism (Scheme 3) has been proposed to explain the kinetic data. This involves the *cis* and *trans* isomers of [Pt(amino acid)(DMSO)Cl], the ionic species [Pt(amino acid)Cl_2]$^-$ and [Pt(amino acid)$(DMSO)_2$]$^+$ and eight trigonal-bipyramidal five-coordinate intermediates. Four of these serve as intermediates for Cl^- exchange or displacement of L by Cl^- and the other four are intermediates for L exchange or displacement of Cl^- by L. Vertically adjacent pairs of these intermediates in this scheme can also be interconverted by a pseudorotation process which may involve a 60° turnstile rotation of the $PtCl_2L$ or PtL_2Cl moiety about the Pt–NO plane.

cis-Diamminedichloroplatinum (**5**, X = Cl) is a clinically important anticancer drug that appears to act by binding to DNA and inhibiting repli-

5 6

TABLE 2

Activation parameters for DMSO solvolysis of *cis*- and *trans*-$[Pt(NH_3)_2Cl_2]$ [33]

Isomer	$\Delta H^{\ddagger}$ (kJ mol^{-1})		$\Delta S^{\ddagger}$ (J K^{-1} mol^{-1})	
	UV [a]	NMR [b]	UV	NMR
cis	79.1	82.8	−60.7	−48.5
trans	64.8	70.7	−89.5	−74.1

[a] At 276 nm (*cis*) and 302 nm (*trans*). [b] Time-dependent ^{195}Pt.

cation. Bidentate coordination of DNA to **5** is preceded by hydrolysis of at least one labile chloride ligand. The *trans* isomer (**6**, X = Cl), which binds DNA in a different bifunctional manner is far less cytotoxic. Since DMSO is commonly used to dissolve these platinum(II) complexes prior to biological usage, the solvolysis effects of DMSO have been investigated by time-dependent ^{195}Pt NMR methods.

A study [32] of the *cis* isomer (**5**) identified complexes of type *cis*-$[Pt(NH_3)_2(DMSO)X]X$ and eventually other products such as *cis*-$[Pt(NH_3)(DMSO)_2H_2O]X_2$ and monoammines *cis*-$[Pt(NH_3)(DMSO)X_2]$. The complexes were identified by their ^{195}Pt chemical shifts and $^1J(^{195}Pt,N)$ coupling constants, the latter varying in magnitude between 226 and 345 Hz, depending on the nature of the *trans* group. The rates of solvolysis were in the order *cis*-$[Pt(NH_3)_2Cl] <$ *cis*-$[Pt(NH_3)_2Br_2] <$ *cis*-$[Pt(NH_3)_2I_2]$. More precise kinetic data were obtained from a recent study on both *cis* and *trans* isomers [33] using both ^{195}Pt NMR and optical spectroscopy. The data are contained in Table 2, inspection of which shows an appreciably faster solvolysis rate for the *trans* isomer, presumably due to the greater kinetic *trans*-labilizing effect of the chlorine atom compared with NH_3. Since the dissolution of the *trans* complex (**6**) in DMSO leads to a small amount of the salt $[Pt(NH_3)_2(DMSO)Cl]^+$ as a contaminant, which affects the DNA binding properties of **6**, the use of DMSO for biological studies is discouraged.

The exchange of DMSO and its displacement by bidentate ligands (L–L) such as 2,2′,-bipyridine in the complex *cis*-$[PtPh_2(DMSO)_2]$ (**7**) have been followed by a parallel flow ^{1}H NMR and UV spectrophotometric study

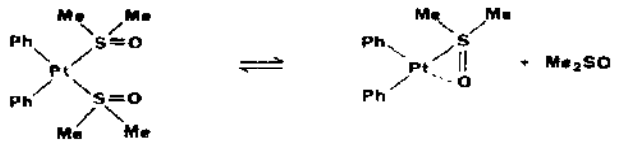

7 8

[34,35]. The main reaction path to $[PtPh_2(L–L)(DMSO)]$ and $[PtPh_2(L–L)]$ was shown to be dissociative, with the reaction intermediate $[PtPh_2(DMSO)]$ (**8**). This species is a result of the strong *trans* influence of the Ph group which weakens and lengthens the Pt–S bond and brings about an appreciable Pt · · · O interaction.

The shorter time scale of ^{195}Pt NMR compared with ^{1}H and ^{13}C (Table 1) arises from the very large chemical shift spread of ^{195}Pt signals. While this feature means that in principle rather fast rate processes can be detected, in practice the utility of ^{195}Pt as a nuclide for DNMR studies may be reduced on account of the excessive coalescence broadening causing the signals to be virtually undetectable. However, if chemical shift differences are very small, as in subtly different diastereoisomeric pairs of species, rate processes may be measured which could remain undetected by less environmentally sensitive nuclei. This point is demonstrated by Kostic and coworkers [36,37] in studies of platinum(II) thioether complexes of type $[PtCl_3(thioether)]^-$. The thioethers used were *N*-formyl-DL-homomethionine, *N*-acetyl-L-methionine (AcMetH), *N*-acetyl-*S*-methyl-DL-cysteine, DL-3-(methylthio)-1,2-propanediol and DL-3-(methylthio)-2-butanone. Each of these complexes exists as almost equally abundant diastereoisomeric forms, which are related by intramolecular inversion of configuration of the coordinated sulphur atom. The two structures of $[PtCl_3(AcMetH)]^-$ are shown (**9** and **10**).

9 10

^{195}Pt spectra changed from two signals at low temperature (about 280–290 K) to a single signal at about 365 K. The chemical shift differences between the signals were small by ^{195}Pt standards, varying from 5 to 34 ppm. Both ^{195}Pt signals exhibited typically large temperature coefficients, the signals moving to high frequency with increasing temperature. Fortunately, the chemical shift differences remained approximately constant, enabling $\Delta G^{\ddagger}$ data, based on coalescence temperature measurements, to be calculated. Values were in the range 64–70 kJ mol^{-1} for coalescence temperatures (T_c) in the range 338–370 K.

(b) Bidentate ligands

Platinum(II) complexes of acyclic sulphides and selenides have been extensively studied by DNMR methods, and activation energies for pyra-

midal chalcogen inversion in both *cis* and *trans* complexes of the type [PtX(L–L)] have been reported previously [7].

The hybrid ligands $RSCH_2C(CF_3)_2O^-$ ($R = CH_3$ or C_6H_5) form *cis* complexes with platinum(II). Five-membered chelate rings are formed by coordination through the "hard" alkoxy and "soft" thioether donor sites. Complexes are of three types: neutral $[Pt\{RSCH_2C(CF_3)_2O\}_2]$ (**11**); neutral $[PtCl\{RSCH_2C(CF_3)_2O\}PPh_3]$ (**12**); cationic $[Pt\{RSCH_2C(CF_3)_2O\}L_2]^+$ ($L = PPh_3$, PPh_2Me, $PPhMe_2$ or PMe_3) (**13**). Variable-temperature ^1H and ^{19}F

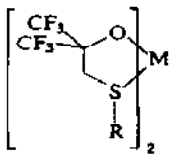

11

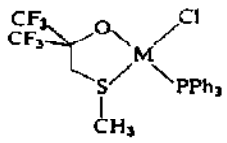

12

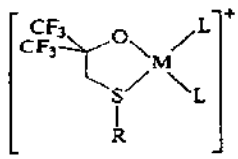

13

NMR enabled sulphur inversion barriers of the thioether function to be evaluated [38,39]. This was achieved by observing both the coalescence of the ligand CH_2 proton resonance from an AB pattern at low temperatures to a singlet (plus ^{195}Pt satellites) at about 90 °C and the coalescence of the two CF_3 fluorine signals. Approximate rate constants were deduced from coalescence temperature measurements and $\Delta G^{\ddagger}$ values (accurate to ± 1 kJ mol^{-1}) estimated. Magnitudes for the cation complexes **13** were in the narrow range 65–68 kJ mol^{-1}, implying little dependence of the R substituent on sulphur or on the nature of the phosphine ligand L. However, a comparison of $\Delta G^{\ddagger}$ data for neutral and ionic complexes shows that the value for **12** is 82 ± 1 kJ mol^{-1}, implying an appreciably larger *trans* effect for PR_3 than for Cl.

X-ray crystal structures of two of the cationic complexes (**13**, $L = PPh_3$, PPh_2Me) showed the five-membered chelate rings to have similar conformations with the CH_3S and axial CF_3 groups in an *anti* conformation [40]. An examination of the ^{19}F NMR spectra of these complexes at temperatures where sulphur inversion is slow supports the notion that the complexes maintain a preferred conformation in solution but that thioether inversion induces complete ring inversion to occur.

Sulphur inversion barrier energies have been used as measures of relative *trans* effects in fluorinated alkoxides of platinum(II). Some new *cis*

platinum(II) complexes of perfluoropinacol $[-OC(CF_3)_2C(CF_3)_2O-]^{2-}$ (PFP) with phosphine and thioether ligands have been synthesized [41]. The general formula is $[(PFP)PtL_2]$ (L = phosphines, SMe_2, MeSEt, SEt_2, S-bonded DMSO; $L_2 = MeS(CH_2)_2SMe$). ^1H, ^{19}F and ^{31}P NMR measurements, particularly values of $^1J(Pt,P)$ in the phosphine complexes, enabled static *trans* influences of the fluorinated alkoxy groups to be estimated for the first time. The order was found to be $Cl^- < -C(CF_3)_2O^- \approx Br^- < I^-$. However, ^1H DNMR studies on the monodentate and bidentate thioether complexes indicated that $-C(CF_3)_2O^-$ had a dynamic *trans* influence less than that of Cl^-, i.e. it is more strongly electron withdrawing than Cl^-. This apparent contradiction has been explained by arguing that platinum(II) forms bonds to alkoxides with a higher degree of electrostatic character and a lower degree of covalent character than those to chloride.

Bis(sulphide) derivatives of ferrocene $Fe(C_5H_4SR)_2$ (R = Ph, ^{i}Pr, ^{i}Bu) can act as bidentate ligands towards palladium(II) and platinum(II), forming *cis* complexes of general type $[Fe(C_5H_4SR)_2MX_2]$ (X = Cl, Br) [42]. These species have interesting stereodynamic possibilities arising from pyramidal inversion of the sulphur atoms and inversion (reversal) of the –S–Pt–S– bridge, as occurs in [3]-ferrocenophanes [43]. Variable-temperature ^1H NMR studies in the range from −60 to 60 °C showed the predominance of a single solution species which underwent a single type of fluxional rearrangement [44]. A total of eight "static" species is possible, and these may be represented as the eight corners of a cubic graph diagram (Scheme 4). Sulphur inversion interconverts species on the front or rear faces of the cube while bridge reversal interconverts adjacent species on the front and rear faces. The ^1H spectra are most reasonably explained by assuming that bridge reversal (BR) is always rapid on the ^1H NMR shift time scale, and that the DL species are dominant. The *meso*-2 form is not observed in any of the complexes, owing to severe steric interactions between the R groups, and the *meso*-1 form is present in low abundance (less than 15%) in the (R = ^{i}Bu) complexes.

The spectral changes are thus primarily associated with interconversion of the DL pair of invertomers (**14** and **15**). This can be monitored accurately by

14 **15**

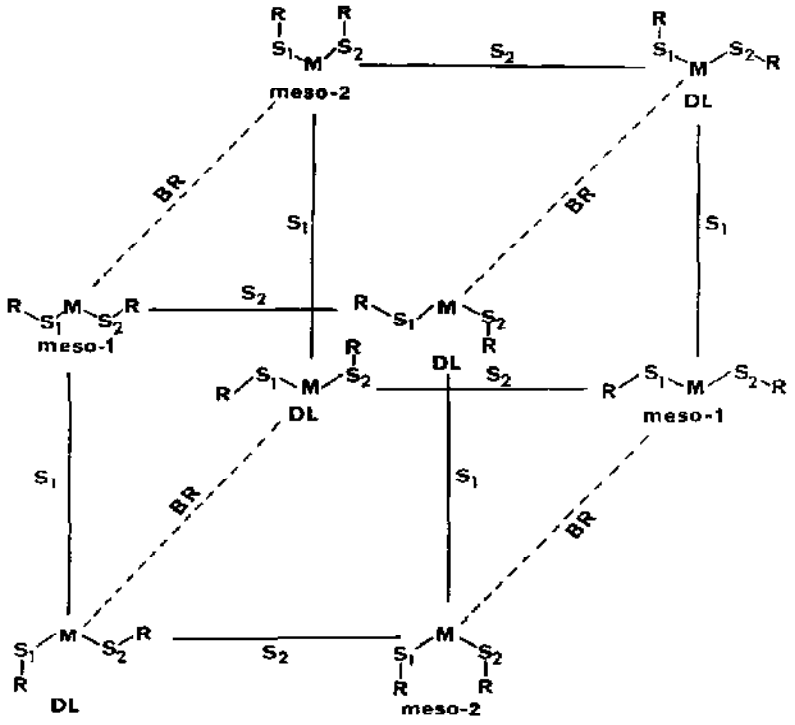

Scheme 4.

the ring methine protons which constitute a dynamic ABCD ⇌ BADC spin system. Total bandshape analysis yielded rate constants from which accurate Eyring energy data were obtained (Table 3). Inspection of the $\Delta G^{\ddagger}$ values shows that the chloride complexes have higher values than the bromide complexes by 0.7–1.9 kJ mol^{-1}, reflecting the greater *trans* influence of Br compared with Cl, with a concomitant weakening of the Pt–S bond. In the $PtBr_2$ series of complexes, $\Delta G^{\ddagger}$ (kJ mol^{-1}) values are 55.8 (R = Ph), 66.0 (R = ^{i}Pr) and 63.1 (R = ^{i}Bu), a trend substantiated for the palladium(II) complexes. The low value for the SPh derivative clearly results from ligand

TABLE 3

Activation energies for sulphur inversion in $Fe(C_5H_4SR)_2PtX_2$ complexes [44]

X	R	$\Delta G^{\ddagger}$(298.15 K) (kJ mol^{-1})
Br	Ph	55.8 ± 0.4
Cl	^{i}Pr	66.7 ± 0.05
Br	^{i}Pr	66.0 ± 0.1
Cl	^{i}Bu	65.0 ± 0.05
Br	^{i}Bu	63.1 ± 0.1

$(3p-2p)\pi$ conjugation between the phenyl ring and the sulphur atom being more effective in the planar transition state of sulphur than in the pyramidal ground state. The slight decrease in $\Delta G^{\ddagger}$ on going from ^{i}Pr to ^{i}Bu suggests that the inversion barrier is less affected by the mass or size of R than by steric factors.

Support for the assumption of rapid –S–Pt–S– bridge reversal may be found in the isolobal theory of Hoffmann [45]. The rate of bridge reversal depends essentially on the torsional barriers of the bridge bonds. In the compound $Fe(C_5H_4S)_2CH_2$ the bridge reversal barrier is low ($\Delta G^{\ddagger} = 47.2$ kJ mol^{-1}) [46] compared with that in $Fe(C_5H_4S)_2S$ where it is high (80.4 kJ mol^{-1}) [43]. This mirrors the difference in torsional energies of S–S and C–S bridge bonds. A d^8 MX_2 moiety is isolobal with CH_2 in frontier orbital terms, and thus it is reasonable to expect a $>Pt^{II}X_2$ moiety in the centre of the three-atom bridge to exert a similar electronic influence on the bridge reversal fluxion as a central CH_2 group. Clearly in the present complexes its influence is slightly greater than that of CH_2 since the dynamic process is now too rapid for detection on the ^{1}H NMR time scale, i.e. $\Delta G^{\ddagger}$ must be less than about 35 kJ mol^{-1}. This suggests a smaller torsional barrier for Pt–S bonds than for C–S bonds.

Reaction of $Li\{CH(PPh_2S)_2\}$ with $[Pt_2Cl_4(PEt_3)_2]$ in tetrahydrofuran gave the C,S-bonded complex **16** which then isomerized to **17** [47].

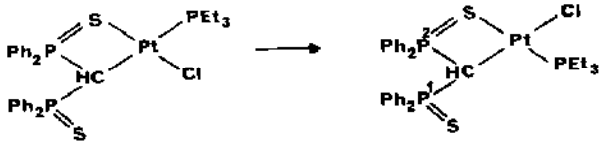

The ambient-temperature $^{31}P-\{^{1}H\}$ spectrum of **17** showed a doublet ($^{2}J(Pt,P) = 301$ Hz) which on cooling to about $-55\,^{\circ}C$ split into two signals due to the phosphorus atoms P^1 and P^2. Clearly, at ambient temperature a rapid dynamic interchange is occurring between coordinated and uncoordinated sulphur atoms. The complex is chiral at the CH carbon atom and the apparent metal–ligand pivot process, which is essentially rotation about the Pt–C bond, inverts the configuration of the complex. Isomer **16**, in contrast, appears to be static at room temperature. Raising its temperature mainly effects isomerization to **17** but there is also evidence of a similar metal–pivot process occurring.

The related S,S-bonded chelate $[PtCl(PEt_3)\{C(PPh_2S)_3\}]$ (**18**) also exhibits unusual stereodynamics at temperatures above about 50 °C [48].

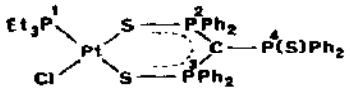

$^{31}P-\{^1H\}$ spectra demonstrate that $S{=}P^4$ exchanges with $S{=}P^3$, but the P^2 signal remains unaffected. Bandshape fittings gave a $\Delta G^{\ddagger}$ value of 67.1 kJ mol^{-1} for this process, which again may be considered to be a Pt–S pivot about the bond *trans* to Cl. The differing bond strengths of Pt–S (*trans* Cl) and Pt–S (*trans* P) are reflected in the bond lengths of 2.282 Å and 2.341 Å, and ^2J(Pt,P) values of 128 Hz and 48 Hz respectively. Similar dynamic effects were observed for related ionic complexes, the notable difference being that both Pt–S bonds are labilized by *trans* phosphine ligands and all three P=S groups are involved in the exchange.

Interaction of the double ylides RR′N–P(X)=NR (R = ^{t}Bu, R′ = $SiMe_3$,

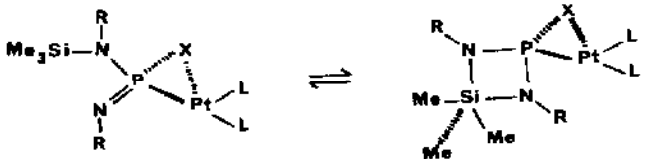

19 20

X = S, Se) with $[(Ph_3P)_2Pt(C_2H_4)]$ affords the P,X-bonded platinum complexes, **19**, with η^2-coordination of the P=X group [49]. Variable-temperature NMR studies showed that the X = S complex is stereochemically non-rigid and at low temperatures the structure **20** with pentacoordinate silicon is favoured.

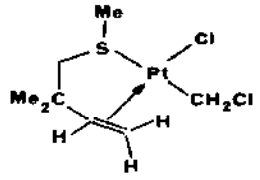

21

Treatment of dichloro(2,2-dimethyl-3-buten-2-yl methyl sulphide)-platinum(II) with diazomethane gives the carbene insertion product **21** [50]. This is a C,S-chelate complex which in $CDCl_3$ solution exhibits pyramidal sulphur inversion. This process causes exchange broadening in the ^{13}C and ^1H spectra of the complex at ambient temperatures. Cooling to either 0 °C (^{13}C) or −30 °C (^1H) revealed signals due to the separate invertomers, but no inversion energy was reported.

Pyramidal sulphur inversion is slow on the NMR time scale at ambient temperatures in platinum(II) halide complexes of chelating polyfluoroalkyldithioethanes such as $CF_3SCH_2CH_2SCF_3$ and $CF_3SCH_2CH_2SCH_3$ [51]. Warming these complexes to about 400 K produces coalescence effects in their ^{19}F NMR spectra owing to appreciable rates of sulphur inversion. Analysis of the ambient-temperature ^{19}F spectra identified isomeric mixtures of complexes with *anti* isomers predominating for the ligand

$CF_3SCH_2CH_2SCF_3$ (**22a** and **22b**) and *anti–syn* isomers dominant for the ligands $CH_3SCH(CF_3)CH_2SCH_3$ and $CF_3SCH(Me)CH_2SCF_3$ (**23a** and **23b**).

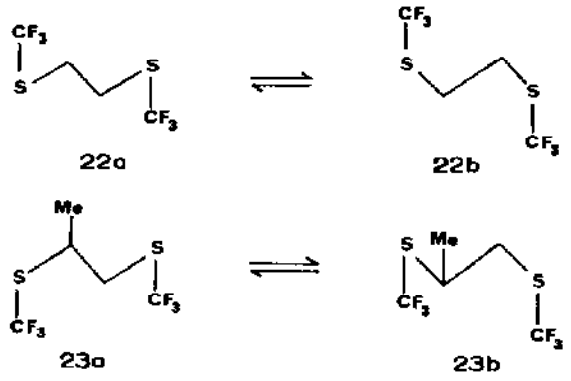

In these cases the five-membered ring puckering process was always fast on the ^{19}F NMR time scale and pseudoplanarity could be assumed. However, in the complex *cis*-$[PtI_2\{CH_3SCH(CF_3)CH(CF_3)SCH_3\}]$ the chelate ring becomes "frozen" in a non-planar geometry owing to restricted rotation about the C–C ligand backbone bond. The evidence for this is provided by the complex ^{19}F spectrum at 183 K. An X-ray crystal structure of the dichloro analogue of the above complex shows that in the crystalline state the chelate ring adopts a conformation intermediate between envelope and symmetrically puckered geometries [52]. In the related complex, *cis*-$[PtCl_2$-*cis*$\{CH_3SCH_2CH(CF_3)SCH_3\}]$, four isomers are detected in solution, the most abundant with the S-methyl groups mutually *syn* and the CF_3 substituent pseudo-equatorial with respect to the chelate ring. The solid state structure of this complex corresponds to this isomer [53].

(ii) Platinum(IV) complexes

The vast majority of the DNMR studies reported in this section are of complexes of the *fac* trimethylplatinum(IV) halide tetramer $[(PtXMe_3)_4]$. This tetrameric structure involving six-coordinate platinum atoms and three-way halogen bridge bonds can be cleaved by sulphur or selenium donors to produce mononuclear and dinuclear platinum(IV) complexes.

(a) Monodentate ligands

Ligands such as dimethyl sulphide or dimethyl selenide can form stable complexes such as $[PtXMe_3(EMe_2)_2]$ (X = Cl, Br or I) and studies of chalcogen inversion in such species have been reported previously [7]. Because of the *fac* geometry at platinum, bidentate chelate complexes of $PtXMe_3$ are more widespread than monodentate complexes, and indeed no new studies of the latter have appeared during the period covered in this review.

(b) Bidentate chelate ligands

Mononuclear platinum(IV) complexes of the general type $[PtXMe_3L]$ (X = Cl, Br or I; L = S or Se chelate donor) comprise an interesting group of fluxional species. With aliphatic dithioethers, diselenoethers, or thioselenoethers as ligands, stable complexes are formed which, in organic solvents at low temperatures, exist as mixtures of invertomers due to the slow rates of pyramidal inversion of the coordinated chalcogen atoms as detected by NMR. The static solution structures and chalcogen inversion characteristics of these complexes have been extensively studied by variable-temperature ^1H and ^{195}Pt NMR and reviewed in 1984 [7]. During the period of this review new developments in this area are as follows.

The ligand 2,4,6-trithiaheptane $MeSCH_2SCH_2SMe$ (L) forms stable chelate complexes of the type $[PtXMe_3L]$ (X = Cl, Br or I) [54]. These six-membered ring complexes are closely related to the complexes $[PtXMe_3\{MeS(CH_2)_3SMe\}]$ where sulphur inversion was detected and measured from changes in the –SMe region of their ^1H NMR spectra. In the present complexes the non-coordinated sulphur atom simplifies the ^1H spectra and allows the pyramidal inversions of the two coordinated sulphur atoms to be followed by changes in the ring methylene, the S-methyl and Pt-methyl regions of the spectra. The sulphur inversion process interconverts the methylene proton environments of the *meso*-1, DL and *meso*-2 in-

TABLE 4

Invertomer populations of $[PtXMe_3L]$ complexes in solution

L	X	E	T (°C)	Solvent	% Population			Ref.
					meso-1	DL	*meso*-2	
$MeSCH_2SCH_2SMe$	Cl	S	−62.2	CD_2Cl_2–CS_2	25.6	62.8	11.6	54
	Br	S	−61.8	CD_2Cl_2–CS_2	27.4	61.6	11.0	54
	I	S	−76.5	CD_2Cl_2–CS_2	34.3	55.2	10.5	54
MeSCH=CHSMe	Cl	S	−76	CD_2Cl_2	74.6	9.8	15.6	55
	Br	S	−76	CD_2Cl_2	63.7	11.0	25.3	55
	I	S	−76	CD_2Cl_2	45.6	17.8	36.6	55
MeSeCH=CHSeMe	Cl	Se	−76	CD_2Cl_2	51.8	17.2	31.0	55
	Br	Se	−76	CD_2Cl_2	40.5	22.4	37.1	55
	I	Se	−76	CD_2Cl_2	17.8	24.0	58.2	55
$MeSCH_2CH_2SMe$	Cl	S	−40	$CDCl_3$	59.5	38.0	2.5	24
	I	S	−40	$CDCl_3$	27.5	62.3	10.2	24
$^tBuSCH_2CH_2S^tBu$	Cl	S	−70	CD_2Cl_2	47.3	47.5	5.2	56
	Br	S	−70	CD_2Cl_2	31.0	59.6	9.4	56
	I	S	−70	CD_2Cl_2	16.8	68.2	15.0	56

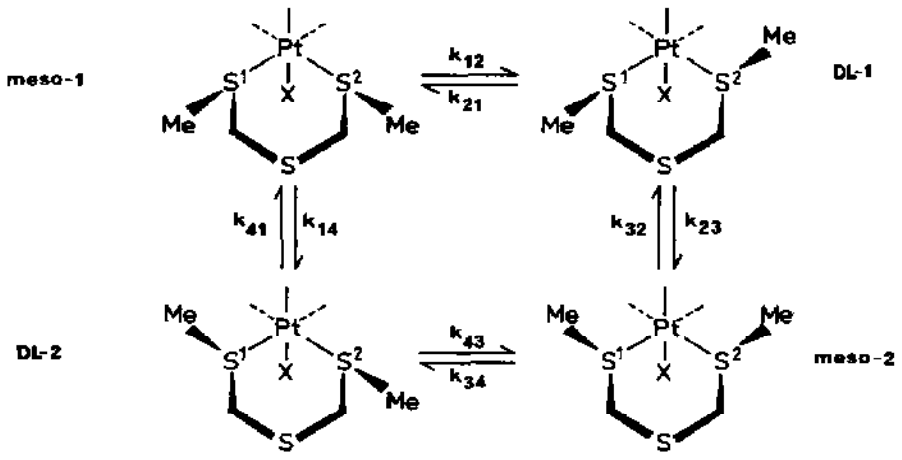

Scheme 5.

vertomers (Table 4) according to Scheme 5. The dynamic spin problem for the methylene protons is thus

$$\begin{array}{ccccc} AB & \rightleftharpoons & CD & & ABX & \rightleftharpoons & CDX \\ \Vert & & \Vert & + & \Vert & & \Vert \\ EF & \rightleftharpoons & GH & & EFX & \rightleftharpoons & GHX \\ & 66.6\% & & & & 33.4\% & \end{array} \qquad X = {}^{195}Pt$$

in the absence of measurable ^4J(H,H) values. It is clear that even when sulphur inversions are rapid the geminal methylene protons have different averaged chemical shifts, namely ⟨ACGE⟩ and ⟨BDHF⟩. Thus the methylene signals change from four AB patterns at low temperatures to a single averaged AB pattern at ambient temperatures when sulphur inversion is rapid. Bandshape analysis of these changes led to precise energy data for the sulphur inversion process, $\Delta G^{\ddagger}$ values measured at 298.15 K being in the range 55.5–58.5 kJ mol^{-1} for the X = Cl and X = Br complexes (Table 5). When the complexes are warmed above ambient temperatures, further fluxionality occurs which averages the methylene proton shifts to a single shift at about 120 °C, and simultaneously the axial and equatorial Pt-methyl environments are exchanged. These changes can only be rationalized by assuming 180° ligand rotations ("pancake flips") which proceed via highly non-rigid eight-coordinate platinum(IV) intermediates which produce Pt-methyl scrambling. The observation of ^{195}Pt satellites to either side of the S-methyl signal at temperatures when the ligand fluxion is rapid confirms the non-dissociative intramolecular nature of this fluxion. Energy data for the fluxional changes deduced separately from the methylene and Pt-methyl regions of the spectra were identical within experimental error (Table 6),

TABLE 5

$\Delta G^{\ddagger}$(298.15 K) data for chalcogen inversion in mononuclear [$PtXMe_3L$] complexes

L	X	E	Process	$\Delta G^{\ddagger}$(298.15 K) (kJ mol^{-1})	Ref.
$MeSCH_2SCH_2SMe$	Cl	S	*meso*-1 → DL	55.71 ± 0.12	54
			DL → *meso*-2	58.00 ± 0.14	
$MeSCH_2SCH_2SMe$	Br	S	*meso*-1 → DL	56.36 ± 0.06	54
			DL → *meso*-2	58.42 ± 0.10	
MeSCH=CHSMe	Cl	S	*meso*-1 → DL	52.4 ± 0.3	55
			DL → *meso*-2	48.1 ± 0.4	
MeSCH=CHSMe	Br	S	*meso*-1 → DL	53.4 ± 0.1	55
			DL → *meso*-2	48.6 ± 0.5	
MeSCH=CHSMe	I	S	*meso*-1 → DL	53.8 ± 0.8	55
			DL → *meso*-2	47.8 ± 0.8	
MeSeCH=CHSeMe	Br	Se	*meso*-1 → DL	63.4 ± 0.1	55
			DL → *meso*-2	60.1 ± 0.1	
$MeSCH_2CH_2SMe$	Cl	S	*meso*-1 → DL	63.40 ± 0.05	24
			DL → *meso*-2	62.14 ± 0.44	
$MeSCH_2CH_2SMe$	I	S	*meso*-1 → DL DL → *meso*-2	62.74 ± 0.13	24
$^tBuSCH_2CH_2S^tBu$	I	S	*meso*-1 → DL DL → *meso*-2	43.33 ± 0.17	56
$MeSCH_2CH_2SEt$	Cl	S(Et)	DL-1 → DL-2	61.3 ± 0.03 [a]	56
		S(Me)	DL-2 → DL-3	62.5 ± 1.2 [a]	
		S(Et)	DL-3 → DL-4	56.1 ± 0.49 [a]	
		S(Me)	DL-1 → DL-4	64.5 ± 0.94 [a]	
$MeSCH_2CH_2SEt$	Br	S(Et)	DL-1 → DL-2	61.6 ± 0.03 [a]	56
		S(Me)	DL-2 → DL-3	64.0 ± 2.2 [a]	
		S(Et)	DL-3 → DL-4	57.7 ± 0.36 [a]	
		S(Me)	DL-1 → DL-4	65.2 ± 2.2 [a]	
$MeSCH_2CH_2SEt$	I	S(Et)	DL-1 → DL-2	61.10 ± 0.04	57
		S(Me)	DL-2 → DL-3	65.4 ± 0.3	
		S(Et)	DL-3 → DL-4	58.2 ± 0.1	
		S(Me)	DL-1 → DL-4	64.4 ± 0.2	
$MeSCH_2CH_2S^tBu$	Cl	S(^{t}Bu)	DL-1 → DL-2	43.21 ± 0.36	56
		S(^{t}Bu)	DL-3 → DL-4	43.56 ± 1.31	
		S(Me)	DL-1/2 → DL-3/4	62.39 ± 0.04	
$MeSCH_2CH_2S^tBu$	I	S(^{t}Bu)	DL-1 → DL-2	43.37 ± 0.73	56
		S(^{t}Bu)	DL-3 → DL-4	44.90 ± 0.40	
		S(Me)	DL-1/2 → DL-3/4	63.47 ± 0.04	
$(MeS)_2CHCH(SMe)_2$ [b]	Cl	S_2	DL-1 → DL-2	56.05 ± 0.09	58
		S_2	DL-3 → DL-4	55.20 ± 0.09	
		S_1	DL-1/2 → DL-3/4	64.56 ± 0.01	
$(MeS)_2CHCH(SMe)_2$ [b]	Br	S_2	DL-1 → DL-2	56.73 ± 0.05	58
		S_2	DL-3 → DL-4	54.34 ± 0.04	
		S_1	DL-1/2 → DL-3/4	63.95 ± 0.01	
$(MeS)_2CHCH(SMe)_2$ [b]	I	S_2	DL-1 → DL-2	56.22 ± 0.04	58
		S_2	DL-2 → DL-3	55.54 ± 0.06	
		S_1	DL-1/2 → DL-3/4	64.83 ± 0.02	

[a] Values at 243 K. [b] *Trans* isomer.

TABLE 6

$\Delta G^{\ddagger}$(298.15 K) data for ligand fluxionality in [$PtXMe_3L$] complexes

L	X	Process [a]	$\Delta G^{\ddagger}$(298.15 K) (kJ mol^{-1})	Ref.
$MeSCH_2SCH_2SMe$	Cl	LR	77.7 ± 0.3	54
		PMS	79.2 ± 0.2	
	Br	LR	78.0 ± 0.8	54
		PMS	79.2 ± 1.5	
	I	LR	78.1 ± 1.0	54
		PMS	79.2 ± 0.4	
MeSCH=CHSMe	Cl	PMS	80.4 ± 0.1	55
MeSeCH=CHSeMe	Br	PMS	79.7 ± 0.1	55
$MeSCH_2CH_2SMe$	I	PMS	89.6 ± 0.3	56
$MeSCH_2CH_2SEt$	Cl	PMS(eq_1–ax)	96.3 ± 0.9	56
		PMS(eq_2–ax)	93.9 ± 0.6	56
		PMS(eq_1–eq_2)	100.4 ± 0.7	56
	I	PMS(eq_1–ax)	92.6 ± 0.4	57
		PMS(eq_2–ax)	90.9 ± 0.5	57
		PMS(eq_1–eq_2)	97.7 ± 1.9	57
$MeSCH_2CH_2S^tBu$	Cl	PMS(eq_1–ax)	89.5 ± 1.2	56
		PMS(eq_2–ax)	80.8 ± 0.4	56
		PMS(eq_1–eq_2)	89.3 ± 0.8	56
$(MeS)_2CHCH(SMe)_2$	Cl	PLP	90.6 ± 0.5	59
		PMS	90.6 ± 0.5	
	Br	PLP	91.2 ± 0.5	59
		PMS	90.1 ± 0.5	
	I	PLP	90.6 ± 0.5	59
		PMS	89.9 ± 0.5	

[a] LR = 180° ligand rotations ("pancake flips"). PMS = Pt-methyl scrambling. PLP = 1,3-Pt–ligand pivoting.

implying that the ligand rotation and Pt-methyl scrambling processes are concerted and are best described as consecutive aspects of a single, extensive fluxional movement.

In order to examine whether π-electron conjugation influences the rates of chalcogen inversion, trimethylplatinum(IV) halide complexes with olefinic thio and seleno ethers were synthesized [55]. Complexes of the general type [$PtXMe_3$(MeECH=CHEMe)] (E = S or Se; X = Cl, Br or I) were examined in CD_2Cl_2 solutions at low temperatures by ^1H, ^{77}Se and ^{195}Pt NMR spectroscopy. The complexes exist as *meso*-1, DL and *meso*-2 invertomer mixtures (Table 4), analogous to the trithiaheptane complexes. The invertomer species differ considerably in their static NMR parameters, particularly in their ^{195}Pt shifts which vary by up to 300 ppm between the three invertomers. Correlations were found between the ^{195}Pt and ^{77}Se shifts, and

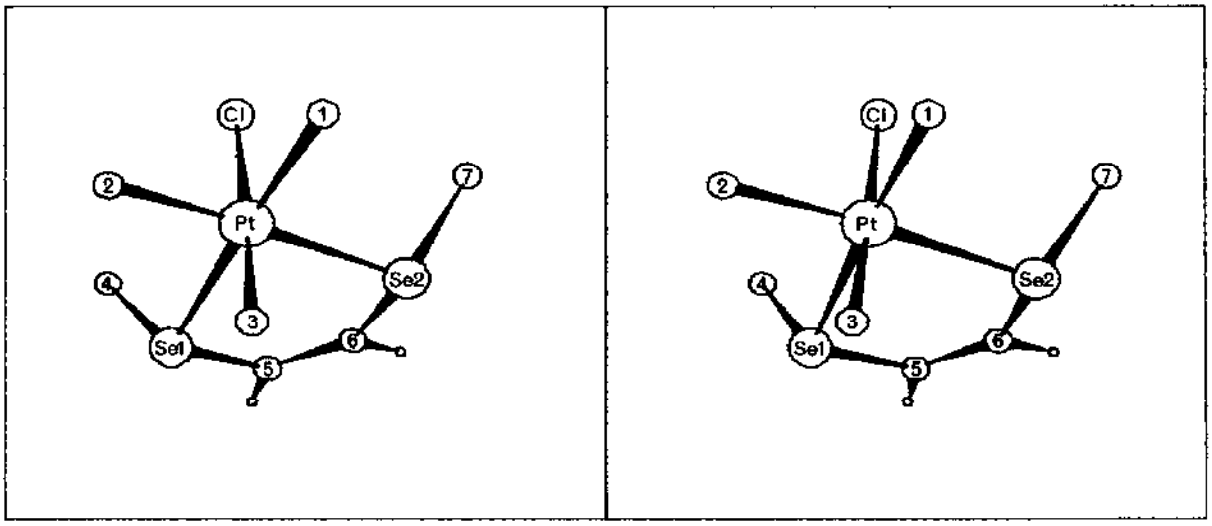

Fig. 1. Stereoview of X-ray structure of [$PtClMe_3$(MeSeCH=CHSeMe)].

between ^{195}Pt and ^{1}J(Pt,Se) values. Increasing the electronegativity of the halogen produced deshielding of the magnetic environments with a corresponding decrease in ^{1}J(Pt,Se) values. However, the latter parameter did not directly reflect the strength of the Pt–Se bond. Invertomer populations varied considerably with the halogen (Table 4), the *meso*-1 isomer becoming less predominant as the halogen size increased. It is also notable that in these olefinic complexes, in contrast with the saturated ligand analogues, the

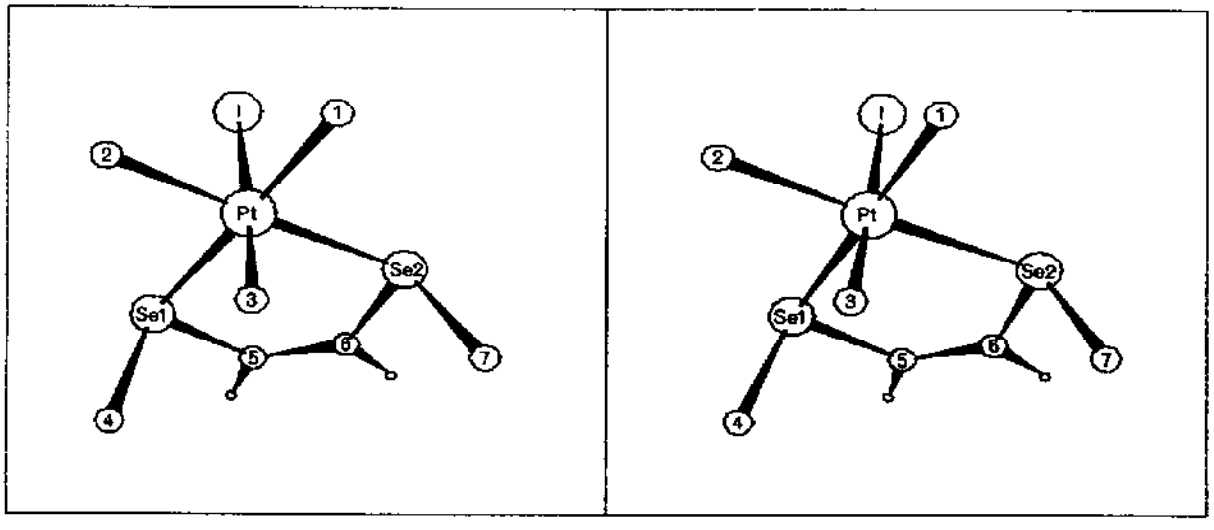

Fig. 2. Stereoview of X-ray crystal structure of [$PtIMe_3$(MeSeCH=CHSeMe)].

DL species are least favoured [24]. In the diselenoether complexes, *meso*-1 is dominant for the chloro complex but *meso*-2 predominates in the iodo complex. This trend is reflected in the solid state structures of these complexes (Figs. 1 and 2), where the ligand geometries are analogous to those of the dominant CD_2Cl_2 solution species. Chalcogen inversion barriers were deduced from variable-temperature ^1H NMR spectra of the methyl signals, and activation energies are given in Table 5. Values are virtually halogen independent but, for sulphur inversion, are 9–14 kJ mol^{-1} lower than for the saturated aliphatic ligand complexes [24]. This is attributed to $(3p-2p)\pi$ conjugation between the chalcogen lone pair and the ligand backbone, with the interaction being more effective in the planar transition state for the inversion than in the ground state. The energy barrier for selenium inversion is about 10 kJ mol^{-1} higher than for the corresponding sulphur inversion, in agreement with previous findings [7]. At above-ambient temperatures, Pt-methyl fluxionality occurs with energies (Table 6) similar to those for the trithiaheptane complexes. With these olefinic ligand complexes it is not possible to detect any ligand rotation movement, but it is presumed to be the precursor of the Pt-methyl fluxion.

The foregoing studies of pyramidal inversion have been directed towards complexes with symmetries such that their DNMR spectra are sensitive to no more than two rate constants, and so 1D NMR bandshape analysis can be employed. With complexes of the type $[PtXMe_3(RSCH_2CH_2SR')]$ (R,R′ = dissimilar alkyl groups) more than two rate constants are required to describe the pyramidal sulphur inversion, and bandshape analysis becomes impracticable. However, it has been mentioned earlier (Section B(iv)) that multisite exchange problems are more effectively dealt with by 2D-EXSY NMR methods. This approach was therefore adopted, but only after it had been thoroughly tested on the complexes $[PtXMe_3(MeSCH_2CH_2SMe)]$ (X = Cl, I) for which reliable rate data, based on 1D bandshape analysis, were already available. These data refer to *meso*-1–DL–*meso*-2 exchange as already described (Scheme 1). The rate data based on ^{195}Pt 2D-EXSY spectra [24] were in excellent accord with the data based on ^1H bandshape analysis. A combination of both sets of data enabled accurate rate constants to be calculated over a temperature range of 110 °C. Using the Eyring rate theory, very accurate $\Delta G^{\ddagger}$ values were deduced for the sulphur inversion processes (Table 5). The 2D method, as opposed to the 1D method, showed conclusively that synchronous double sulphur inversion was negligible since rate constants for this process were explicitly calculated to be zero within experimental accuracy.

Having demonstrated the quantitative reliability of the 2D-EXSY NMR method for three-site exchange problems, Abel et al. applied it to the four-site exchange associated with sulphur inversion in the complexes

$[PtXMe_3(RSCH_2CH_2SR')]$ (X = Cl, Br or I; R = Me, R' = Et or ^tBu) [56,57]. The stereodynamics of these species are intractable by conventional 1D bandshape analysis on account of the complexities of their low temperature ^1H spectra arising from the four distinct invertomers DL-1, DL-2, DL-3 and DL-4. These are shown in Scheme 6, together with the exchange pathways arising from single-site and double-site inversion. It will be seen that the inversion dynamics are governed by six independent forward rate constants which are not deducible by 1D bandshape analysis but may be directly derived from relative signal intensities in ^{195}Pt 2D-EXSY spectral maps. The case of $[PtIMe_3(MeSCH_2CH_2SEt)]$ [57] is illustrated in Fig. 3. The 1D spectrum above the 2D contour map shows the assignment of the different invertomer species. The relative populations of these invertomers are very temperature and halogen dependent. For example, at 223 K, the DL-4 invertomer is dominant for the iodo complexes, the ordering being DL-4 > DL-2 > DL-1 > DL-3 (Table 7). However, increasing the electronegativity of the halogen favours DL-1 at the expense of the other invertomers, leading to the following ordering for the chloro complexes, namely DL-1 > DL-4 > DL-2 > DL-3. This change-over in populations also occurs, for the iodo complexes, on raising the temperature to ambient values. Analysis of the ^{195}Pt 2D-EXSY spectra using the D2DNMR program [24] enabled the six rate constants defining the inversion process to be explicitly calculated. The two rate constants k_{13} and k_{24} for the synchronous double-inversion process were

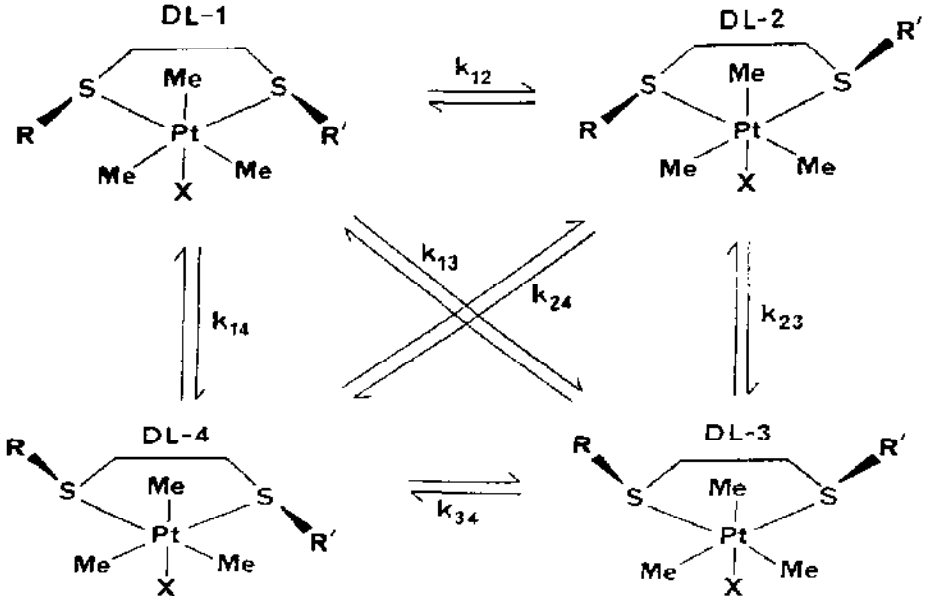

Scheme 6.

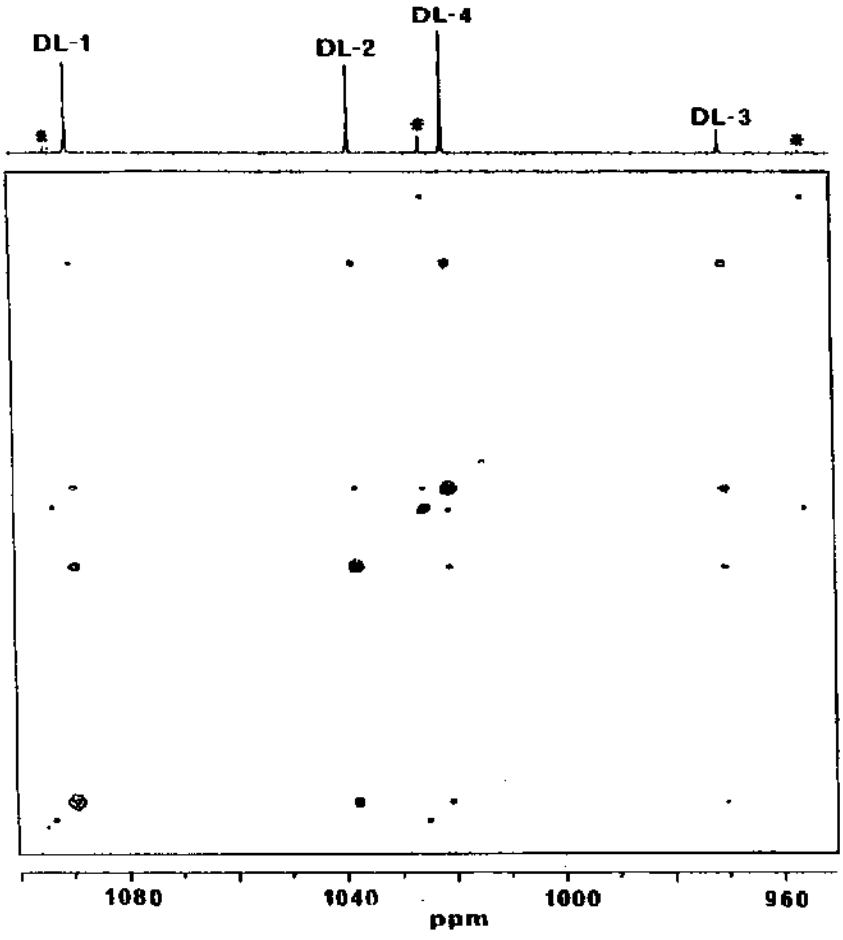

Fig. 3. ^{195}Pt 2D-EXSY NMR spectrum of [$PtIMe_3(MeSCH_2CH_2SEt)$] ($CDCl_3$ solution, 263 K, $\tau_m = 0.08$ s). Signals marked with an asterisk are due to a small amount of [$PtIMe_3(MeSCH_2CH_2SMe)$].

again zero within experimental accuracy. The other rate constants enabled the energy barriers for the four single-inversion pathways to be deduced (Table 5). Two of these (DL-1 → DL-2, DL-3 → DL-4) refer to S-ethyl inversion and the other two (DL-2 → DL-3, DL-1 → DL-4) refer to S-methyl inversion. By combining the results of both studies [56,57], the following definitive trend in S-alkyl inversion barriers was obtained, namely SMe (about 64 kJ mol^{-1}) > SEt (about 60 kJ mol^{-1}) ≫ S^{t}Bu (about 45 kJ mol^{-1}). This finding is in accord with studies of nitrogen inversion in which the steric strain of a bulkier group is relieved somewhat in the transition state, the energy of which (relative to the ground state) becomes lower than that for less sterically hindered species.

High temperature fluxionality also occurs in these unsymmetrical di-

TABLE 7

Invertomer populations of [$PtXMe_3L$] complexes in solution

L	X	T (°C)	Solvent	% Population				Ref.
				DL-1	DL-2	DL-3	DL-4	
$MeSCH_2CH_2SEt$	Cl	−30	$CDCl_3$	53.0	20.7	2.9	23.3	56
	Br	−30	$CDCl_3$	41.1	24.0	5.9	28.6	56
	I	−30	$CDCl_3$	26.0	27.4	10.5	36.1	57
$MeSCH_2CH_2S^tBu$	Cl	−70	CD_2Cl_2	39.4	21.8	3.9	34.9	56
	Br	−70	CD_2Cl_2	25.9	24.3	6.6	43.2	56
	I	−70	CD_2Cl_2	15.8	25.7	11.3	47.2	56
$(MeS)_2CHCH(SMe)_2$ [a]	Cl	−30	$CDCl_3$	27.9	34.5	4.8	4.4	58
	Br	−30	$CDCl_3$	20.4	46.7	8.5	4.7	58
	I	−30	$CDCl_3$	12.9	55.2	12.8	7.1	58

[a] *Trans* isomer.

thioether complexes. The employment of 2D NMR methods again provides greater insight into the mechanisms of this fluxionality. In these complexes the three Pt-methyl environments are dissimilar in the absence of any rapid fluxion, and thus using proton 2D-EXSY experiments the three-site exchange may be closely monitored and separate rates for equatorial–equatorial (eq–eq) exchange and the two types of axial–equatorial (ax–eq) exchange derived. It will be seen (Table 6) that the associated $\Delta G^{\ddagger}$ data for these exchanges are measurably different. Ligand 180° rotations will effect eq–eq exchange only, whereas scrambling of the Pt-methyl environments either by a random mechanism or by some type of concerted movement will exchange all three methyl sites. Thus any uncorrelated combination of these processes will result in the rate of eq–eq exchange at any temperature being greater than ax–eq exchange. This is the opposite to what is observed and so a concerted ligand rotation with a Pt-methyl exchange mechanism is implied. Since Pt-methyl bond breaking does not occur, the exchange of axial and equatorial Pt-methyl environments is thought to occur by 120° rotations of the $PtMe_3$ moiety about its C_3 axis. If these movements were precisely correlated with 180° ligand rotations, then no net eq–eq exchange would occur. A graph diagram depicting the six permutational isomers of the complex illustrates the problem (Fig. 4). Correlated ligand 180°/$PtMe_3$ 120° rotations interchange the six species with rate constants k_{13} or k_{23} depending on which Pt-methyl is exchanged in a particular step. It would appear that these pathways are most favoured energetically. However, some direct eq–eq exchange does occur, at a somewhat slower rate (Table 6), and thus the other pathways in Fig. 4 are also traversed. In other words, strongly

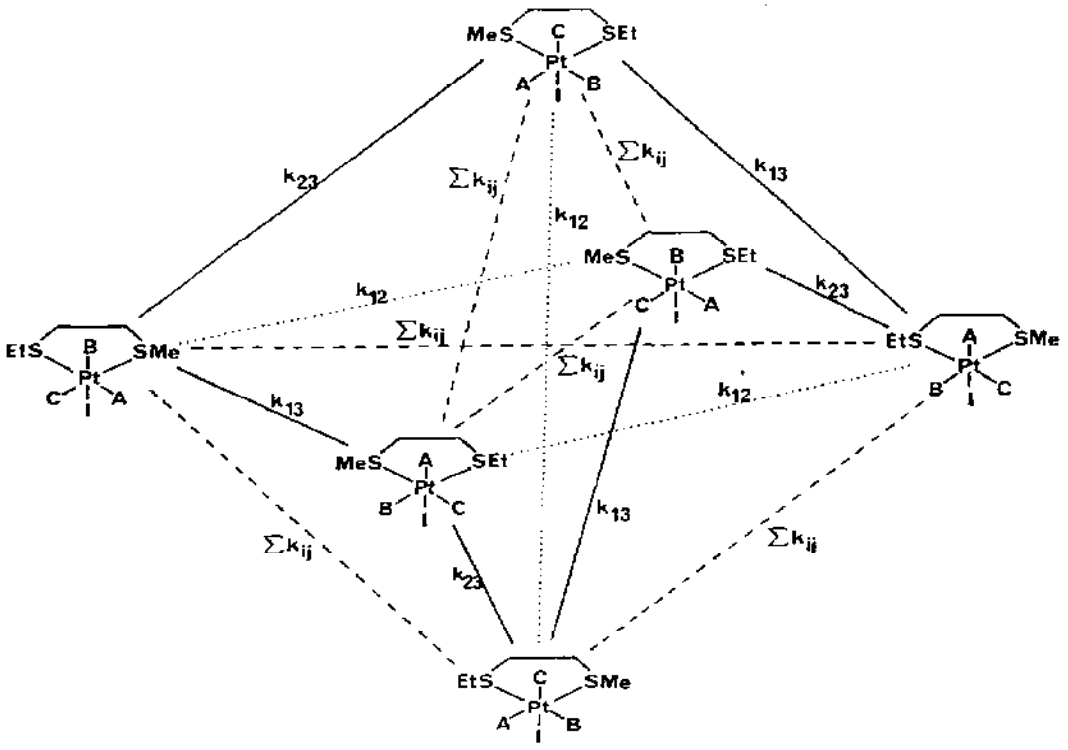

Fig. 4. Graph diagram showing the interconversion pathways of the six permutational isomers of $[PtIMe_3(MeSCH_2CH_2SEt)]$. Pathways are defined as (———) correlated ligand (180°)/ $PtMe_3$ (120°) rotations, (- - - - - -) $PtMe_3$ 120° rotations, (· · · · · ·) ligand 180° rotations. Rate constants are defined according to Scheme 6.

correlated ligand 120°/$PtMe_3$ 120° rotation occurs together with some uncorrelated movements. In the case of the $[PtXMe_3(MeSCH_2CH_2S^tBu)]$ complexes there appears to be a lower degree of correlation between the ligand-centred and $PtMe_3$-centred movements (Table 6).

The ligand 1,1,2,2-tetrakis(methylthio)ethane, $(MeS)_2CHCH(SMe)_2$ (L), provides interesting possibilities for coordination with $[(PtXMe_3)]_4$, since both mononuclear $[PtXMe_3L]$ and binuclear $[(PtXMe_3)_2L]$ complexes are likely products. Both types of complexes have recently been obtained but the ligand preferentially acts as a chelate forming mononuclear species [58]. These can exist as configurational isomers *cis*-1 (**24**), *cis*-2 (**25**) and a *trans* DL pair (**26a** and **26b**). The *trans* isomers predominate (more than 70% at 243 K) and only one of the *cis* isomers, presumed *cis*-1, is detected in $CDCl_3$ solution. The ordering of invertomer populations of the *trans* isomer is DL-2 > DL-1 > DL-3 > DL-4 but abundances are very halogen dependent (Table 7). The invertomer numbering follows that employed for the $RSCH_2CH_2SR'$ ligand complexes, the DL-2 invertomer being most favoured

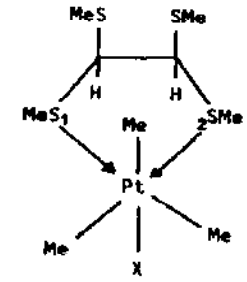

24

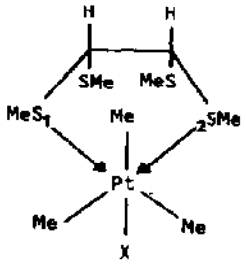

25

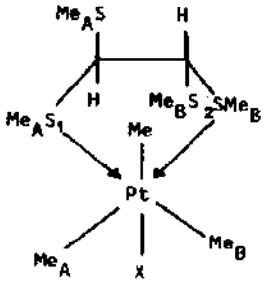

26a

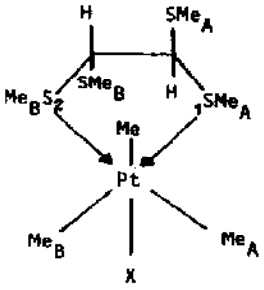

26b

since in this species the two uncoordinated S-methyl groups are both *trans* to each other and also *trans* to their contiguous coordinated S-methyl groups. The X-ray crystal structure of $[PtIMe_3(MeS)_2CHCH(SMe)_2]$ is compatible with this ligand conformation [58].

Sulphur inversion in these complexes was followed by bandshape analysis of the methine proton signals, which changed from four AB quartets at low temperatures to two averaged AB quartets at high temperatures. Inversion energy data (Table 5) showed that inversion at the S_2 sulphur occurs more readily than at the S_1 sulphur. The difference in $\Delta G^{\ddagger}$ values is around 9 kJ mol^{-1}, which corresponds to S_2 inverting 40–50 times faster than S_1 at any temperature. This is attributed to a slight weakening of the Pt–S_2 bond by the interaction of the halogen with the *cis* uncoordinated S-methyl.

The high temperature fluxionality of these complexes is particularly novel [59]. Hydrogen spectra measured in the temperature range 333–423 K showed exchange between all Pt-methyl environments and between all coordinated and uncoordinated S-methyl groups. Exchange of all S-methyl environments implies *trans* ⇌ *cis*-1 isomer exchange and this process was followed by ^1H bandshape analysis of the methine region and ^1H 2D-EXSY studies of the S-methyl region. Results were in good agreement and mean values are quoted in Table 6.

The bandshape analysis method was based on the interconversion

trans ⇌ *cis*-1

⇅ ⇅

cis-2 ⇌ *trans* *

where *trans* / *trans* * form an enantiomeric pair. The mechanism of this interconversion can be envisaged as a 1,3-pivoting process, which involves rearrangements of individual Pt–S bonds with 109.5° (tetrahedral angle) pivots of the pendent $-CH(SMe)_2$ group about its attached C–C bond. This movement brings the previously uncoordinated *gem* S-methyl into coordination with the platinum atom. Such a process causes *trans–cis* interconversion, accompanied by simultaneous exchange of coordinated and uncoordinated *gem* S-methyl groups. By a sequence of two Pt-S_1/S_1' and S_2/S_2' rearrangements the four isomers can be produced (Scheme 7). However, *cis*-2 was undetected and, furthermore, the bandshape fittings showed that there was negligible direct *trans* ⇌ *trans* * exchange. Thus the fluxional process was

trans ⇌ *cis*-1 ⇌ *trans* *

and may be described as a reciprocating clockwise–anticlockwise pivot about the ligand C–C bond. A similar type of 1,3-metal pivot process has

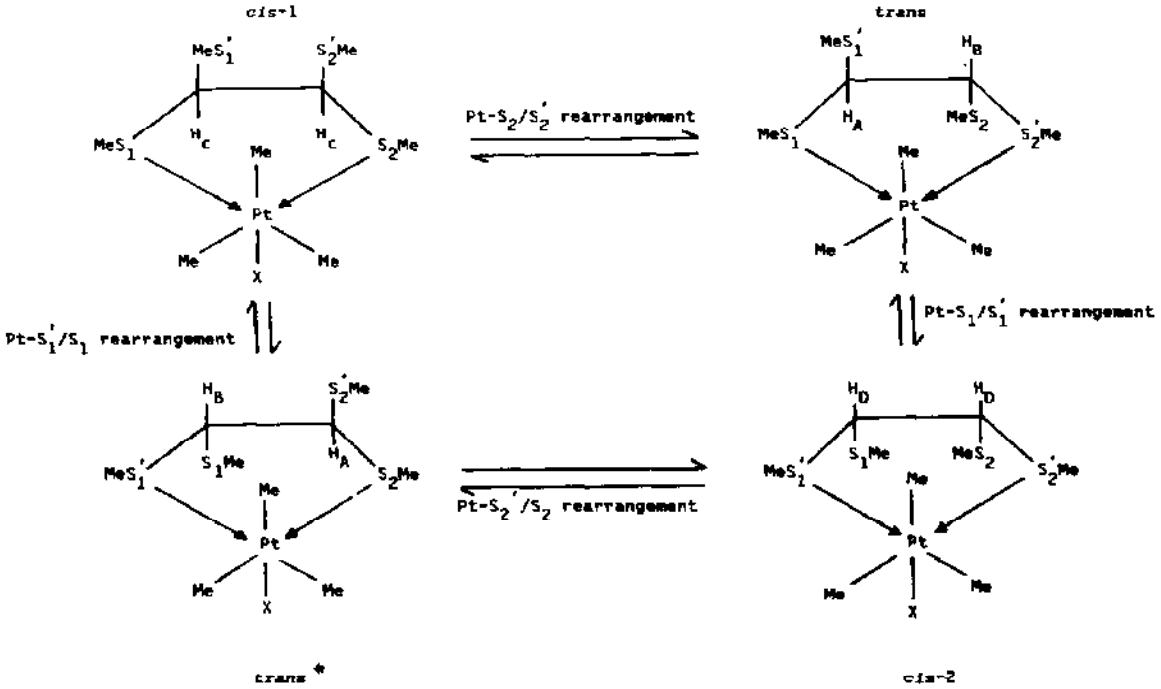

Scheme 7.

been detected in binuclear platinum(IV) complexes [7] but is hitherto unknown in mononuclear platinum(IV) analogues.

As in the other $[PtXMe_3L]$ complexes, Pt-methyl exchange accompanies the ligand fluxions mentioned above. Activation energies derived from ^1H 2D-EXSY spectra of the Pt-methyl signals are identical with the ligand pivoting energies within experimental accuracy (Table 6), indicating that the two processes are strongly correlated and share a common transition state.

(c) Bidentate bridging ligands

Binuclear platinum(IV) complexes of type $[(PtXMe_3)_2L]$ are formed between $[(PtXMe_3)_4]$ and acyclic or cyclic ligands (L) when the latter possess no more than one carbon atom between the potential donor sites. Thus binuclear complexes are formed when L = $MeECH_2EMe$, MeEEMe, (E = S or Se), MeSSeMe, $\overline{SCH_2SCH_2SCH_2}$ and $\overline{SCHMeSCHMeSCHMe}$ [7]. In all these complexes the ligand bridges the two platinum(IV) atoms which are also linked by two halogen bridge bonds.

A more recent study [60] has been concerned with the eight-membered ring ligand 1,3,5,7-tetrathiocane, $\overline{SCH_2SCH_2SCH_2SCH_2}$. The platinum(IV) complex has the structure shown in Fig. 5. At temperatures around $-25\,^\circ C$ the ^1H NMR spectra of these complexes indicate "static" species with the methylene signals comprising an AB quartet (for the bridging methylene)

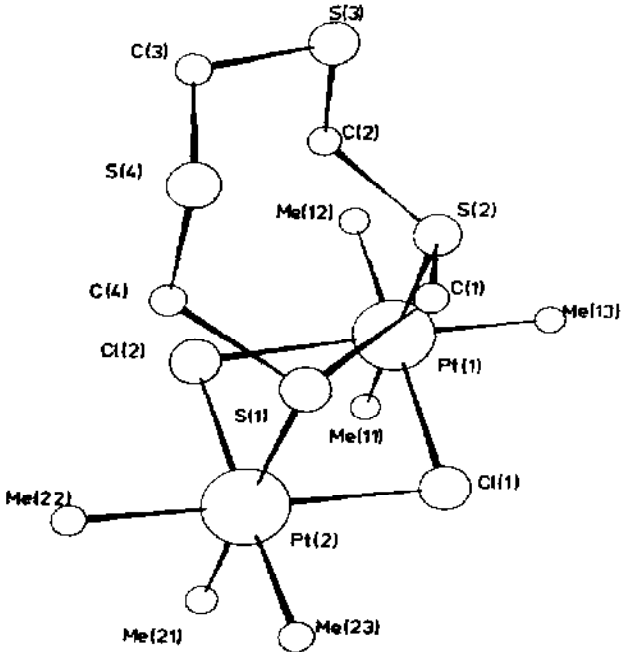

Fig. 5. The X-ray crystal structure of $[(PtClMe_3)_2(\overline{SCH_2SCH_2SCH_2SCH_2})]$.

and two singlets. On warming the complexes, exchange broadening occurred and coalescence of all signals was achieved at about 15°C. By analogy with complexes of 1,3,5-trithian, $\overline{SCH_2SCH_2SCH_2}$ [7,20], this effect was thought to be a consequence of the binuclear platinum moiety commuting over all sulphur atoms by a series of 1,3-pivots about any one S–Pt bond. However, the additional uncoordinated sulphur atom of the tetrathiocane ligand also allows the fluxion to proceed via a six-coordinate intermediate species rather than a seven-coordinate transition state. The alternative mechanisms are depicted in Fig. 6. Mechanism A closely allies that proposed for the trithian complexes, the main difference being that it comprises a 90° 1,5-pivot as opposed to a 60° 1,3-pivot. Mechanism B entails the formation of a 1,5-coordinate intermediate species, followed by a series of 1,3-pivots about either coordinated sulphur atom. The net result is that one or both platinum atoms change their coordination sites by two sequential 45° 1,3-pivots. A careful analysis of the methylene proton bandshapes provides unequivocal support for mechanism A, and accurate $\Delta G^{\ddagger}$ data for the process were reported (Table 8). Analysis of the bandshape changes in the Pt-methyl region of the ^1H spectra gave very similar $\Delta G^{\ddagger}$ values (Table 8), suggesting another case of a concerted ligand pivoting and Pt-methyl exchange mechanism. A detailed analysis of the rate data showed that a mechanism involving clockwise or anticlockwise 120° rotations of the pivot-commuting $PtMe_3$ moiety about its cone axis can fully explain the NMR findings. Thus the overall mechanism consists of 90° 1,5-metal pivots with 120° rotations

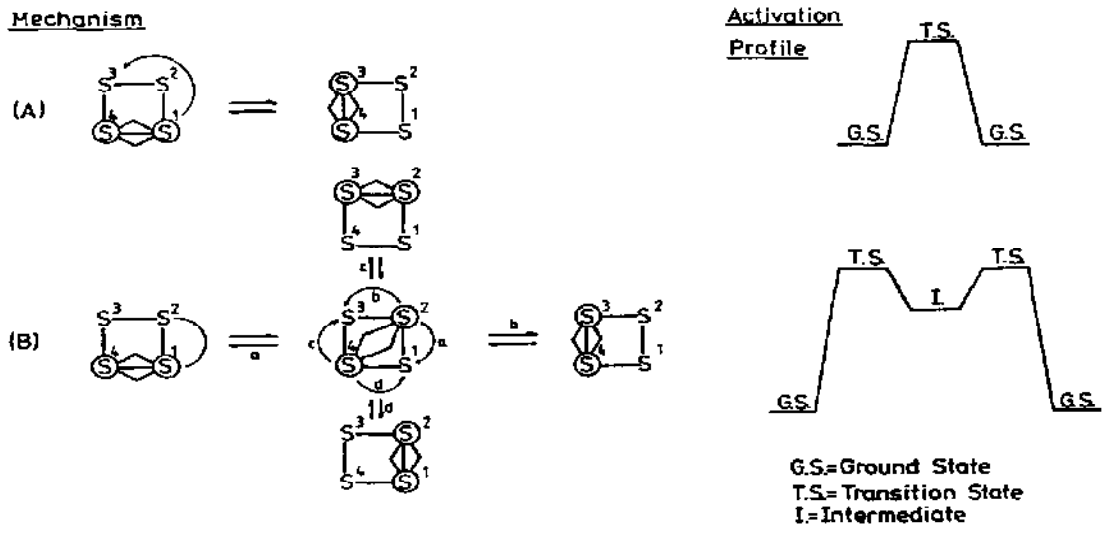

Fig. 6. Alternative mechanisms for metal pivoting in binuclear platinum(IV) complexes of 1,3,5,7-tetrathiocane. The numbering of sulphur atoms refers to Fig. 5.

TABLE 8

Activation energies ($\Delta G^{\ddagger}$) for fluxional processes in $[(PtXMe_3)_2L]$ complexes

		Process [a]	$\Delta G^{\ddagger}$(298.25 K) (kJ mol^{-1})	Ref.
$\overline{SCH_2SCH_2SCH_2SCH_2}$	Cl	MP	66.15 ± 0.01	60
		MS	65.82 ± 0.01	
$\overline{SCH_2SCH_2SCH_2SCH_2}$	Br	MP	63.95 ± 0.27	60
		MS	63.90 ± 0.01	
$\overline{SCH_2SCH_2SCH_2SCH_2}$	I	MP	60.55 ± 0.19	60
		MS	59.79 ± 0.03	
$\overline{SCH_2CMe_2S}$	Cl	DSI	66.23 ± 0.02	61, 62
		MS	71.38 ± 0.05	
$\overline{SeCH_2CMe_2CH_2Se}$	Cl	DSeI	74.44 ± 0.18	61, 62
		MS	74.92 ± 0.14	
$HC(SMe)_3$	Cl	SI	45.5 ± 1.3	63
		MP	71.7 ± 0.2	
		MS	71.9 ± 0.1	

[a] MP = metal pivoting; MS = methyl scrambling; DSI = double sulphur inversion; DSeI = double selenium inversion.

of the pendent $PtMe_3$ moieties, both movements involving a single seven-coordinate platinum(IV) transition state.

In earlier studies of dithioethers and diselenoethers coordinated to platinum(IV), pyramidal inversion of the chalcogen atoms involved independent inversion of individual atoms, the rates of synchronous double inversion being negligible. However, if the chalcogen atoms are constrained in a ring, they can invert only in synchronism. The platinum(IV) complexes of the ligands 4,4-dimethyl-1,2-dithiacyclopentane, $\overline{SCH_2CMe_2CH_2S}$, and its selenium analogue were therefore synthesized and examined by variable-temperature NMR [61,62]. The complexes $[(PtXMe_3)_2\overline{ECH_2CMe_2CH_2E}]$ (X = Cl, Br, I; E = S, Se) exhibited static ^1H spectra at ambient temperatures. The methylene region consisted of an AB quartet with the higher frequency component showing ^{195}Pt satellites (^2J = 10–15 Hz). On warming the complexes these signals coalesced (Fig. 7) as did also the ring methyl and the equatorial Pt-methyl groups. This clearly indicated synchronous inversion of the chalcogen pairs, producing a "flapping" of the five-membered ligand ring relative to the $(PtXMe_3)_2$ moiety (Fig. 8). The $\Delta G^{\ddagger}$ values for this process (Table 8) exceed values for single-atom inversion by over 20 kJ mol^{-1}. Double-site inversion is thus an appreciably less favoured process than single-site inversion, and whenever ligands have the choice between these mechanisms, independent inversion of individual pyramidal atoms will predominate. The Pt-methyl exchange occurs in these complexes at rates only slightly lower than those of double inversion (Table 8). However, the

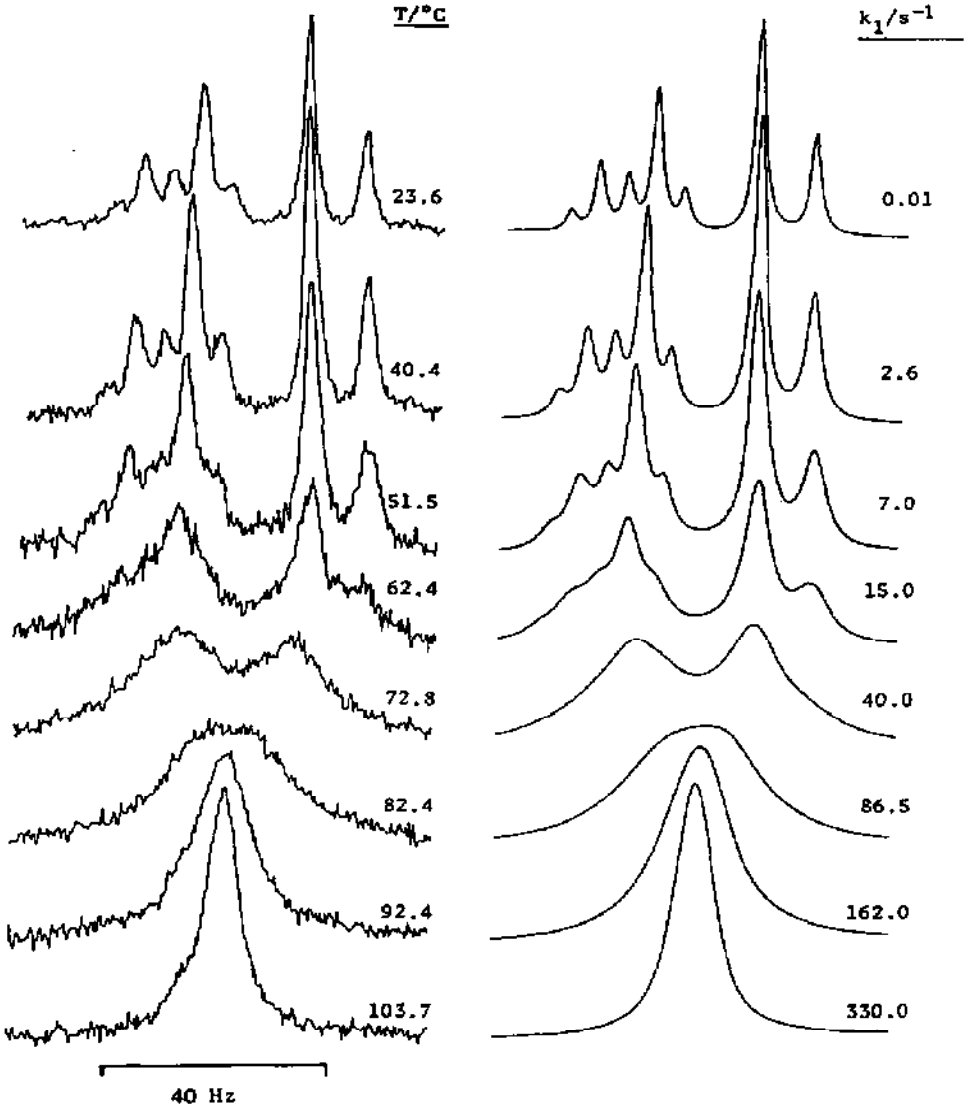

Fig. 7. Experimental and computer synthesized NMR spectra of the ligand methylene region of $[(PtClMe_3)_2(\overline{SeCH_2CMe_2CH_2Se})]$ showing the effects of synchronous selenium inversion.

two processes may be distinguished by analysing the Pt-methyl region of the spectra. It is noteworthy that the $\Delta G^{\ddagger}$ values for this fluxion are 9–10 kJ mol^{-1} higher than for the open-chain ligand complexes $[(PtXMe_3)_2(MeEEMe)]$ [7]. These two series of complexes differ primarily in the degree of distortion of the Pt_2X_2 moiety arising from the mismatching of the ligand bite and the Pt · · · Pt contact distance. This mismatching is very considerable in the present cyclic ligand complexes and is likely to contribute to a higher transition state energy.

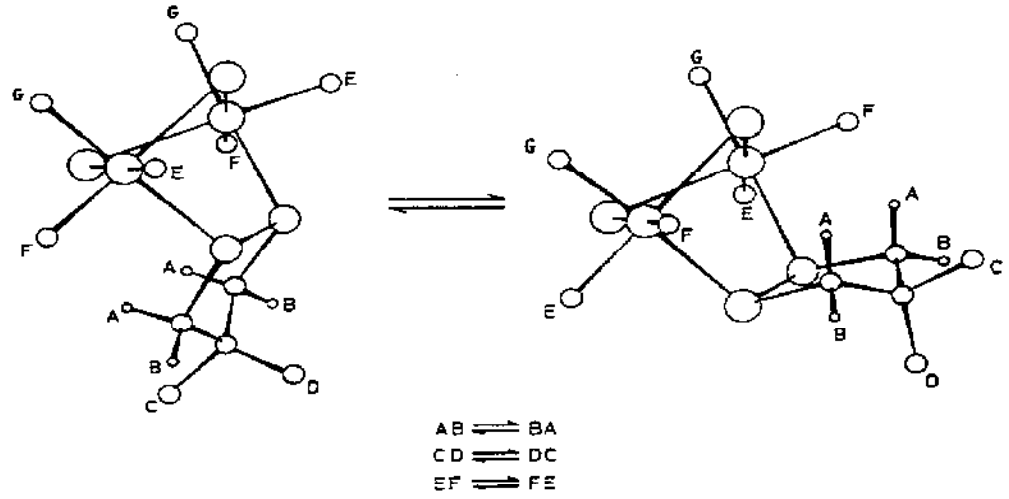

Fig. 8. The effects of synchronous double inversion on the diastereotopic ligand methylene, methyl, and equatorial Pt-methyl environments of $[(PtXMe_3)_2(\overline{ECH_2CMe_2CH_2E})]$. It should be noted that the labelling refers to chemical environments, not atoms. The structures are based on X-ray crystal data. It should also be noted that the ligand five-membered ring will be effectively planar in solution as a result of rapid pseudorotation.

The ligand tris(methylthio)methane, $HC(SMe)_3$, also satisfies the criterion for forming binuclear platinum(IV) complexes, and the species $[(PtXMe_3)_2HC(SMe)_3]$ (X = Cl, Br) (27) were indeed isolated [63]. Their variable-temperature ^1H NMR spectra were analysed in a similar way to

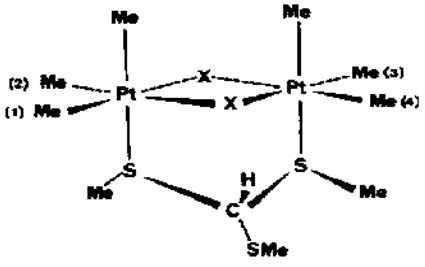

27

those of the tetrathiocane complexes [60]. From bandshape analyses of the S-methyl and Pt-methyl regions, activation energies were derived for pyramidal sulphur inversion, 1,3-metal pivoting and Pt-methyl exchange (Table 8). The similarity of the energies for the last two mentioned processes again suggests a concerted mechanism, in this case involving 60° ligand pivots together with 120° rotations of the pendent $PtMe_3$ moiety about its three-fold axis.

Dimethyl disulphide, MeSSMe, and dimethyl diselenide, MeSeSeMe, form

binuclear platinum(IV) complexes which have been extensively characterized by DNMR methods [7]. More recently the interaction of diphenyl dichalcogens, PhEEPh (E = S, Se or Te), with $[(PtXMe_3)_4]$ has been examined [64]. However, the only binuclear complexes isolated were $[(PtXMe_3)_2(PhTeTePh)]$ (X = Br, I). As is usual in these complexes the ligand adopted a *trans*(DL) conformation. A DNMR study carried out on the iodo complex yielded $\Delta G^{\ddagger}$ data for pyramidal tellurium inversion (59.72 ± 0.09 kJ mol^{-1}) and Pt-methyl exchange (64.54 ± 0.03 kJ mol^{-1}). The tellurium inversion energy should be compared with the selenium inversion value of 53.4 kJ mol^{-1} in $[(PtBrMe_3)_2(MeSeSeMe)]$ and the sulphur inversion value of 40.7 kJ mol^{-1} in $[(PtBrMe_3)_2(MeSSMe)]$ [7]. Thus the order of inversion energies, sulphur < selenium < tellurium, established for platinum(II) complexes [7] is also valid for platinum(IV) complexes. The magnitudes of these values point to their being attributed to independent inversions of individual chalcogen atoms even though the other invertomer (*cis*) was not detected.

All the foregoing binuclear complexes contained halogen bridge bonds between the platinum(IV) atoms. However, $[(PtXMe_3)_4]$ will react with mononuclear metal thiolato complexes such as $[M(dppe)(SMe)_2]$ (M = Pd(II), Pt(II)) to give thiolato-bridged binuclear complexes of type $[M(dppe)(\mu_2\text{-}SMe)_2PtXMe_3]$ [65]. In the solid state the methylthio groups adopt an *anti* arrangement, thereby minimizing steric crowding. In solution at low temperatures (about 180 K) the *anti* configuration is favoured (relative population is greater than 60% for all complexes) but a *syn* configuration with both S-methyl groups *trans* to X is also observed. On warming the complexes to ambient temperatures, sulphur inversion is accelerated, causing the low temperature ^{31}P signals (i.e. AB quartet (*anti*) plus singlet (*syn*)) to broaden and coalesce. Bandshape analysis yielded $\Delta G^{\ddagger}$ data in the range 44–50 kJ mol^{-1}. Values for the Pt(II)–Pt(IV) complexes were slightly lower than for the Pd(II)–Pt(IV) complexes and there was a slight halogen dependence such that I > Br > Cl. Both these trends in pyramidal sulphur inversion energies are unusual and not easily rationalized.

At higher solution temperatures, equilibration of the Pt-methyl environments occurs with $\Delta G^{\ddagger}$ values in the range 77–86 kJ mol^{-1}. Additionally, in the Pd(II)–Pt(IV) complexes the methylthio signal underwent an unexpected bandshape change. At ambient temperature, each methylthio hydrogen is coupled strongly to its *trans* phosphorus atom (^4J(P,H) = 14 Hz) and weakly to its *cis* phosphorus atom (^4J(P,H) < 1 Hz). At higher temperatures, however, equal coupling to both phosphorus atoms is apparent. This is thought to be the result of a rotation of the (dppe Pd(II)) moiety through 180°. This effect is not observed in the Pt(II)–Pt(IV) complexes, implying that any rotation of the (dppe Pt(II)) moiety is slow on the ^{1}H NMR time scale up to about 150 °C. The energies of the Pd(II)-ligand rotation fluxion

are 8–11 kJ mol^{-1} lower than those of the Pt-methyl fluxion, suggesting that the two movements are not concerted and involve different transition states. The net effect of these movements may be visualized as the palladium(II) and platinum(IV) moieties undergoing independent "rotations" relative to the central methylthio bridging groups producing a type of "ball-joint" fluxion (**28a**).

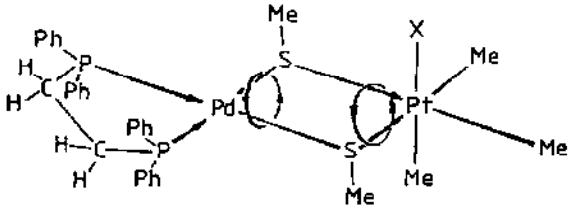

28a

(d) Tridentate ligands

Once the stereodynamics of trimethylplatinum(IV) halide complexes with bidentate thioethers and selenoethers had been established, the effect of introducing a third potential inverting centre was explored using tridentate

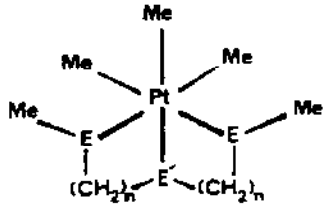

28b

ligands of the type $MeE(CH_2)_nE'(CH_2)_nEMe$ (**28b**) [66]. These form ionic complexes of type $[PtMe_3\{MeE(CH_2)_nE'(CH_2)_nEMe\}]^+X^-$ ($n = 3$, E = E′ = S; $n = 2$, E = S or Se, E′ = O, S or Se; $n = 2$, E = S, E′ = SS; X = I, BPh_4 or BF_4). In the case of the symmetrical tridentate ligand complexes, the chalcogen atoms are centres of chirality so that, in the absence of pyramidal inversion, four diastereoisomers may occur, two distinct *meso* isomers and a DL pair. Inversion at the central chalcogen atom would produce another set of four diastereoisomers, but since there was no evidence for more than one set, this inversion was assumed to be energetically inaccessible. Furthermore, low temperature ^1H NMR spectra indicated the presence of only three out of the four invertomers, no signals due to the sterically crowded *meso*-2 species being detected. In general, the DL-1/2 population was greater than the *meso*-1 population, except in the case of the complex ($n = 3$, E = E′ = S, X = BF_4) where the six-membered rings undergo rapid chair–chair reversal, which disfavours the DL species.

The effects of pyramidal inversion of the terminal chalcogen atoms were quantitatively assessed by bandshape analyses of the S-methyl and equatorial Pt-methyl regions. Excellent fittings were achieved using rate constants for *meso*-1 ⇌ DL-1/2 and DL-1 ⇌ DL-2 exchanges, yielding $\Delta G^{\ddagger}$ data in the range 48–60 kJ mol^{-1} for sulphur inversion and in the range 71–73.5 kJ mol^{-1} for selenium inversion. These barriers were found to depend on the central chalcogen E′ in the order Se ≈ S > O, which is related to the length of the Pt–E bond as reflected in the ^{2}J(Pt,H) coupling constants. The markedly weaker Pt–O bond clearly makes the transition state more accessible.

On heating the complex which has platinum coordinated to a central disulphide group (E′ = SS), a 1,2-metal commutation occurs as shown by the single broad Pt-methyl signal at 155 °C due to Pt-methyl exchange resulting from the highly fluxional pseudo-seven-coordinate intermediate (Scheme 8).

For the complexes containing a centrally coordinated oxygen atom, coalescence of Pt-methyl signals, with retention of ^{195}Pt coupling, occurs more readily. This indicates Pt-methyl scrambling due to the inherent weakness of the Pt–O bond which favours dissociation at high temperatures to produce a stereochemically non-rigid five-coordinate intermediate. Bandshape analysis yielded a $\Delta G^{\ddagger}$ value of 72 ± 0.6 kJ mol^{-1} for this process; this value was more than 15 kJ mol^{-1} lower than values associated with the analogous fluxion in the bidentate dithioether and diselenoether complexes [$PtXMe_3(MeECH_2CH_2E'Me)$] [7] where the transition state is thought to involve eight-coordinate platinum(IV).

The macrocyclic sulphides 1,4,7-trithiacyclononane, 1,4,7,10-tetrathiacyclododecane and 10-oxa-1,4,7-trithiacyclododecane have recently been shown to act as tridentate ligands towards [$(PtClMe_3)_4$] to produce ionic complexes [$PtMe_3L$]Cl [67,68]. In the case of 1,4,7-trithiacyclononane all three sulphur atoms are coordinated in a *fac* endodentate manner to platinum(IV). Similar structures are produced with the other two ligands with either one of the sulphur atoms or the oxygen atom remaining uncoordinated (**29**, E = S, O). Variable-temperature NMR of **29** (E = S) revealed a

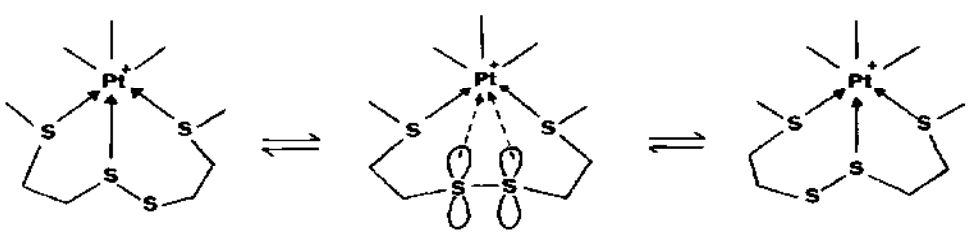

Scheme 8.

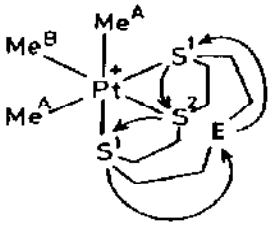

29

fluxionality that produced equilibration of the two Pt-methyl environments (i.e. those *trans* to S^1 and S^2) and a simplification of the methylene region to an AA′BB′ multiplet in the ^1H NMR spectrum and to a single signal in the $^{13}C-\{^1H\}$ spectrum at 333 K. These spectral changes are consistent with an intramolecular ligand pivot mechanism involving a series of correlated 1,4-metallotropic shifts. These are depicted in **29** (E = S). Ligand pivot mechanisms have been referred to earlier in connection with binuclear platinum(IV) complexes of 1,3,5-trithian [7,20], 1,3,5,7-tetrathiocane [60] and tris(methylthio)methane [63]. These fluxions were shown to proceed via either 1,3- or 1,5-metal commutations. Open-chain chalcogen ligand complexes [7] are known to proceed via 1,2- or 1,3-metal shifts, but the fluxionality in this macrocyclic sulphide ligand complex represents the first observation of a 1,4-metallotropic shift in a transition metal complex of a chalcogen ligand. The free energy of activation, $\Delta G^{\ddagger}$(298.15 K), of 56.79 ± 0.02 kJ mol^{-1} is the lowest magnitude to date of any ligand pivot energy. Previous experience of metal pivot fluxions suggests that their activation energies are related to the degree of conformational flexibility of the coordinated ligand. Thus the low $\Delta G^{\ddagger}$ value implies a restricted degree of conformational flexibility in this coordinated macrocycle with the uncoordinated sulphur atom being favourably positioned for participation in the fluxion.

It is noteworthy that the complexes of the other two macrocycles were conformationally rigid in the temperature range from −90 to 60 °C, suggesting that at least one uncoordinated sulphur atom is necessary for the onset of this 1,4-metal commutation.

(iii) Platinum cluster compounds

Syntheses are currently being achieved for an increasing number of metal cluster compounds which incorporate platinum atoms in the metal framework either exclusively or in combination with other metals. In many of these species the oxidation state of the platinum atom(s) is not clearly defined.

When platinum exists in its +4 oxidation state its compounds are almost exclusively octahedral, and in order to retain its six-coordination, novel

bonding is often required. For that reason the trimethylplatinum(IV) halides are tetrameric with three-way halogen bridges, i.e. $[\{PtMe_3(\mu_3\text{-}X)\}_4]$. It has been seen that these tetramers are the precursors for a wide range of fluxional chalcogen coordination complexes. However, some very recent experiments suggest that the tetramers themselves may be undergoing Pt-methyl fluxionality at above-ambient temperatures. Evidence for this comes from the recent isolation of the mixed thiolato- and halogen-bridged tetramers $[(PtMe_3)_2(\mu_3\text{-}SMe)_2(\mu_3\text{-}X)_2(PtMe_3)_2]$ (X = Cl, Br or I) (**30**) [69]. These

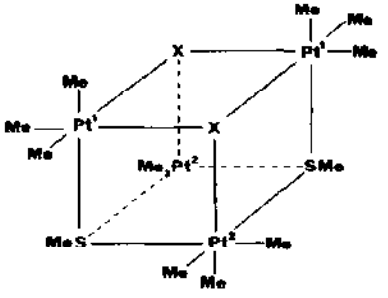

30

species contain two types of $PtMe_3$ moiety each containing two distinct methyl environments (those *trans* SMe and those *trans* X). Exchange between these pairs of methyl environments occurs on warming these complexes. ^1H NMR bandshape analysis of $[(PtMe_3)_2(\mu_3\text{-}SMe)_2(\mu_3\text{-}Cl)_2(PtMe_3)_2]$ yielded $\Delta G^{\ddagger}$ values of 65.6 and 61.3 kJ mol^{-1} for the fluxions, the higher value being associated with the $PtMe_3$ group attached by two halogen and one SMe bridge bonds. Similar fluxionality would seem most likely to exist in the symmetrical tetramers $[\{PtMe_3(\mu_3\text{-}X)\}_4]$ and $[\{PtMe_3(\mu_3\text{-}SR)\}]$ [70]. Unfortunately, the high symmetry of these species precludes any direct NMR observation of fluxionality since all twelve Pt-methyl environments are isochronous and therefore insensitive to any rearrangement.

Triangular clusters of platinum atoms form compounds that possess a total of 42 or 44 electrons. Examples containing Pt–S bonds include $[Pt_3(\mu\text{-}SO_2)_3(PPh_3)_3]$ (42 electrons), and $[Pt_3(\mu\text{-}SO_2)_2(CN^tBu)_5]$ (44 electrons). Interconversion of 42- and 44-electron platinum *triangulo* clusters has been achieved for $[Pt_3(\mu\text{-}SO_2)_3\{P(C_6H_{11})_3\}_3]$ which is converted to $[Pt_3(\mu\text{-}SO_2)_3\{P(C_6H_{11})_3\}_2\{Ph_2P(CH_2)_nPPh_2\}]$ ($n = 2$, 3) (**31**) [71]. The structures

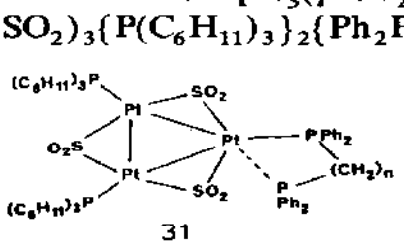

31

were established by X-ray diffraction, and by ^{31}P and $^{195}Pt\text{–}\{^1H\}$ NMR.

The platinum atoms form an approximate isosceles triangle with Pt–Pt distances significantly longer than Pt–Pt distances in comparable platinum clusters. This may be partly due to the large radii of the bridging sulphur atoms. Two of the SO_2 units lie above the plane of the metal triangle and one lies below it. At ambient temperatures, $^{31}P-\{^1H\}$ spectra show three signals (relative intensities 2 : 1 : 1) while the $^{195}Pt-\{^1H\}$ spectra exhibit two signals, a doublet and a doublet of doublets. These observations indicate coordination of the diphosphine ligand to one platinum atom such that its two phosphorus atoms are inequivalent. However, on cooling the complexes, the ^{195}Pt doublet signal broadens to a maximum around 20 °C and eventually splits into two doublets at about −60 °C. The ^{31}P signals also exhibit additional complexity on cooling. These changes suggest an intramolecular flipping process for which a $\Delta G^{\ddagger}$ value of about 45 kJ mol^{-1} was estimated from the $^{195}Pt-\{^1H\}$ spectra.

Triangulo platinum clusters containing the unit $Pt_3(\mu_3\text{-}S)$ serve as models for the poisoning of platinum surfaces with H_2S in heterogeneous catalysis. With this application in mind, the reactions of H_2S and H_2Se with coordinately unsaturated cluster cations $[M_3(\mu_3\text{-}CO)(\mu\text{-}dppm)_3]$ (M = Pt, Pd) have been investigated [72]. Complexes of the general type $[M_3H(\mu_3\text{-}E)(\mu\text{-}dppm)_3][PF_6]$ (M = Pt, E = S, Se; M = Pd, E = S) (**32**) were formed. Variable-temperature ^1H NMR spectra provided evidence that the triply bridged

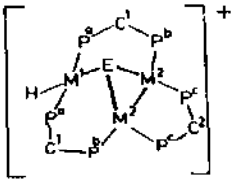

M = Pt, E = S
M = Pt, E = Se

32

sulphur atoms underwent pyramidal inversion which was fast on the NMR time scale at room temperature, producing equivalence of the geminal methylene protons attached to either C^1 or C^2. On cooling to about −80 °C, geminal methylene distinction was achieved and energy data determined. Values were in the range 44–54 kJ mol^{-1} and showed that inversion was more facile with palladium clusters than with platinum clusters. The selenium complex did not show any detectable inversion up to 50 °C, above which decomposition began.

Platinum can be attached to clusters of three or four osmium atoms to form compounds of stoichiometry $PtOs_3(CO)_9(PMe_2Ph)_2(\mu_3\text{-}S)_2$ and $PtOs_4(CO)_{11}(PMe_2Ph)_2(\mu_3\text{-}S)$ [73,74]. The first compound consists of an open triangular cluster of three osmium atoms with a $Pt(PMe_2Ph)_2$ group bridging one of the two Os–Os bonds, whereas the second compound

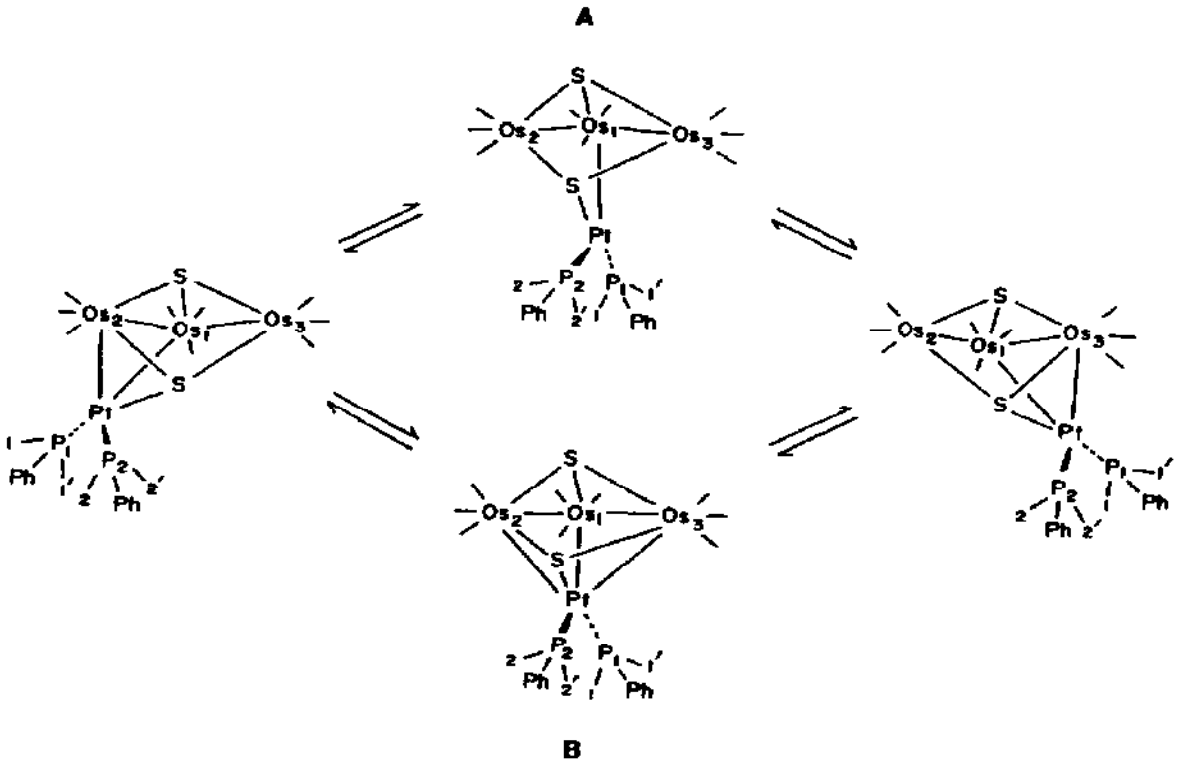

Scheme 9.

consists of a butterfly tetrahedron of four osmium atoms with a $Pt(PMe_2Ph)_2$ group bridging one of the peripheral edges. The $PtOs_3$ cluster undergoes a fluxional rearrangement since the expected non-equivalence of all four methyl groups of the phosphine ligands is only apparent at about 155 K. Above this temperature, their ^1H NMR signals broaden and coalesce in pairs until by about 200 K two sharp signals are observed with ^{31}P coupling. An approximate value of $\Delta G^{\ddagger}$(167 K) of 31.4 kJ mol^{-1} was obtained from the coalescence of one pair of signals. Two possible mechanisms of a dynamic process which can explain the NMR findings have been proposed (Scheme 9). Mechanism **A** involves a bond being formed between platinum and the third osmium atom, whereas in mechanism **B** a Pt–Os bond is broken. The two processes are indistinguishable by NMR, but mechanism **A** is preferred as the intermediate is stable according to the skeletal electron pair (SEP) theory.

REFERENCES

1 E.W. Abel, R.P. Bush, F.J. Hopton and C.R. Jenkins, J. Chem. Soc., Chem. Commun., (1966) 58.

2 C. Brevard and P. Granger, Handbook of High Resolution Multinuclear NMR, Wiley, New York, 1981.
3 J. Mason (Ed.), Multinuclear NMR Spectroscopy, Plenum, New York, 1987.
4 P.S. Belton, I.J. Cox and R.K. Harris, J. Chem. Soc., Faraday Trans. 2, 81 (1985) 63.
5 J.F. Hinton, Annu. Rep. NMR Spectrosc., 19 (1987) 1.
6 M. Baiwir, in F.J. Berry and W.R. McWhinnie (Eds.), Proc. 4th Int. Conf. on Organic Selenium and Tellurium Chemistry, University of Aston, Birmingham, 1983, p. 406.
7 E.W. Abel, S.K. Bhargava and K.G. Orrell, Prog. Inorg. Chem., 32 (1984) 1.
8 E.W. Abel, K.G. Orrell and A.W.G. Platt, Org. Magn. Reson., 21 (1983) 196.
9 E.W. Abel, K.G. Orrell and A.W.G. Platt, J. Chem. Soc., Dalton Trans., (1983) 2345.
10 P.S. Pregosin, Annu. Rep. NMR Spectrosc., 17 (1986) 285.
11 W. Jurinac, J. Chem. Soc., Dalton Trans., (1984) 1537.
12 J. Mason, Chem. Rev., 87 (1987) 1299.
13 E.W. Abel, A.R. Khan, K. Kite, K.G. Orrell and V. Šik, J. Chem. Soc., Dalton Trans., (1980) 1169.
14 E.W. Abel, K.G. Orrell and V. Šik, unpublished work, 1983.
15 R.K. Harris, P. Reams and K.J. Packer, J. Chem. Soc., Dalton Trans., (1986) 1015.
16 J.K.M. Sanders and B.K. Hunter, Modern NMR Spectroscopy, A Guide for Chemists, Oxford University Press, Oxford, 1987, Chapt. 7.
17 R.G. Bryant, J. Chem. Educ., 60 (1983) 933.
18 G. Binsch and D.A. Kleier, Program 140, Quantum Chemistry Program Exchange, Indiana University, IN, 1969.
19 J. Sandström, Dynamic NMR Spectroscopy, Academic Press, London, 1982.
20 K.G. Orrell and V. Šik, Annu. Rep. NMR Spectrosc., 19 (1987) 79.
21 J.K.M. Sanders and J.D. Marsh, Prog. NMR Spectrosc., 15 (1982) 353.
22 B.E. Mann, Chem. Soc. Rev., 15 (1986) 167.
23 R. Willem, Prog. NMR Spectrosc., 20 (1987) 1.
24 E.W. Abel, T.P.J. Coston, K.G. Orrell, V. Šik and D. Stephenson, J. Magn. Reson., 70 (1986) 34.
25 E.W. Abel, A.R. Khan, K. Kite, K.G. Orrell and V. Šik, J. Chem. Soc., Dalton Trans., (1980) 1175.
26 R.J.H. Clark, G. Natile, V. Belluco, L. Cattalini and C. Filippino, J. Chem. Soc. A, (1970) 659.
27 E.W. Abel, M. Booth and K.G. Orrell, J. Chem. Soc., Dalton Trans., (1980) 1582.
28 E.W. Abel, K.G. Orrell, K.B. Qureshi and V. Šik, Polyhedron, 7 (1988) 1321, 1329.
29 E.W. Abel, S.K. Bhargava, T.E. MacKenzie, P.K. Mittal, K.G. Orrell and V. Šik, J. Chem. Soc., Chem. Commun., (1982) 983.
30 E.W. Abel, M. Booth, G.D. King, K.G. Orrell, G.M. Pring and V. Šik, J. Chem. Soc., Dalton Trans., (1981) 1846.
31 L.E. Erickson, T.A. Ferrett and L.F. Buhse, Inorg. Chem., 22 (1983) 1461.
32 S.J.S. Kerrison and P.J. Sadler, Inorg. Chim. Acta, 104 (1985) 197.
33 W.I. Sundquist, K.J. Ahmed, L.S. Hollis and S.J. Lippard, Inorg. Chem., 26 (1987) 1524.
34 S. Lanza, D. Minniti, R. Romeo, P. Moore, J. Sachinidis and M.L. Tobe, J. Chem. Soc., Chem. Commun., (1984) 542.
35 S. Lanza, D. Minniti, P. Moore, J. Sachinidis, R. Romeo and M.L. Tobe, Inorg. Chem., 23 (1984) 4428.
36 D.D. Gummin, E.M.A. Ratilla and N.M. Kostic, Inorg. Chem., 25 (1986) 2429.
37 J.A. Galbraith, K.A. Menzel, E.M.A. Ratilla and N.M. Kostic, Inorg. Chem., 26 (1987) 2073.

38 R.T. Boeré and C.J. Willis, Can. J. Chem., 63 (1985) 3530.
39 R.T. Boeré and C.J. Willis, Can. J. Chem., 64 (1986) 492.
40 R.T. Boeré, N.C. Payne and C.J. Willis, Can. J. Chem., 64 (1986) 1474.
41 R.T. Boeré and C.J. Willis, Inorg. Chem., 24 (1985) 1059.
42 B. McCulloch, D.L. Ward, J.D. Woollins and C.H. Brubaker, Jr., Organometallics, 4 (1985) 1425.
43 E.W. Abel, M. Booth and K.G. Orrell, J. Organomet. Chem., 208 (1981) 213.
44 K.G. Orrell, V. Šik, C.H. Brubaker, Jr., and B. McCulloch, J. Organomet. Chem., 276 (1984) 267.
45 R. Hoffmann, Angew. Chem., Int. Ed. Engl., 21 (1982) 711.
46 E.W. Abel, M. Booth, C.A. Brown, K.G. Orrell and R.L. Woodford, J. Organomet. Chem., 214 (1981) 93.
47 J. Browning, G.W. Bushnell, K.R. Dixon and A. Pidcock, Inorg. Chem., 22 (1983) 2226.
48 J. Browning, K.A. Beveridge, G.W. Bushnell and K.R. Dixon, Inorg. Chem., 25 (1986) 1987.
49 O.J. Scherer, H. Jungmann, C. Krüger and G. Wolmershausen, Chem. Ber., 117 (1984) 2382.
50 R. McCrindle, G. Ferguson, G.J. Arsenault, A.J. McAlees, B.L. Ruhl and D.W. Sneddon, Organometallics, 5 (1986) 1171.
51 R.J. Cross, D.S. Rycroft, D.W.A. Sharp and H. Torrens, J. Chem. Soc., Dalton Trans., (1980) 2434.
52 W.N. Hunter, K.W. Muir and D.W.A. Sharp, Acta Crystallogr. Sect. C, 40 (1984) 37.
53 W.N. Hunter, K.W. Muir and D.W.A. Sharp, Acta Crystallogr. Sect. C, 41 (1985) 1750.
54 E.W. Abel, M.Z.A. Chowdhury, K.G. Orrell and V. Šik, J. Organomet. Chem., 258 (1983) 109.
55 E.W. Abel, S.K. Bhargava, K.G. Orrell, A.W.G. Platt, V. Šik and T.S. Cameron, J. Chem. Soc., Dalton Trans., (1985) 345.
56 E.W. Abel, I. Moss, K.G. Orrell, V. Šik, D. Stephenson, P.A. Bates and M.B. Hursthouse, J. Chem. Soc., Dalton Trans., (1988) 521.
57 E.W. Abel, I. Moss, K.G. Orrell, V. Šik and D. Stephenson, J. Chem. Soc., Dalton Trans., (1987) 2695.
58 E.W. Abel, T.P.J. Coston, K.M. Higgins, K.G. Orrell, V. Šik and T.S. Cameron, J. Chem. Soc., Dalton Trans., (1989) 701.
59 E.W. Abel, T.P.J. Coston, K.G. Orrell and V. Šik, J. Chem. Soc., Dalton Trans., (1989) 711.
60 E.W. Abel, G.D. King, K.G. Orrell, V. Šik, T.S. Cameron and K. Jochem, J. Chem. Soc., Dalton Trans., (1984) 2047.
61 E.W. Abel, P.K. Mittal, K.G. Orrell, V. Šik and T.S. Cameron, J. Chem. Soc., Chem. Commun., (1984) 1312.
62 E.W. Abel, P.K. Mittal, K.G. Orrell and V. Šik, J. Chem. Soc., Dalton Trans., (1986) 961.
63 E.W. Abel, T.E. MacKenzie, K.G. Orrell, and V. Šik, J. Chem. Soc., Dalton Trans., (1986) 2173.
64 E.W. Abel, M.A. Beckett, K.G. Orrell, V. Šik, D. Stephenson, H.B. Singh and N. Sudha, Polyhedron, 7 (1988) 1169.
65 E.W. Abel, N.A. Cooley, K. Kite, K.G. Orrell, V. Šik, M.B. Hursthouse and H.M. Dawes, Polyhedron, 6 (1987) 1261.
66 E.W. Abel, K. Kite and P.S. Perkins, Polyhedron, 6 (1987) 549.
67 E.W. Abel, P.D. Beer, I. Moss, K.G. Orrell, V. Šik, P.A. Bates and M.B. Hursthouse, J. Chem. Soc., Chem. Commun., (1987) 978.

68 E.W. Abel, P.D. Beer, I. Moss, K.G. Orrell, V. Šik, P.A. Bates and M.B. Hursthouse, J. Organomet. Chem., 341 (1988) 559.
69 E.W. Abel, K.G. Orrell and D. Stephenson, J. Organomet. Chem., (1989).
70 E.W. Abel, K. Kite and B.L. Williams, J. Organomet. Chem., 231 (1982) 271.
71 M.F. Hallam, N.D. Howells, D.M.P. Mingos and R.W.M. Wardle, J. Chem. Soc., Dalton Trans., (1985) 845.
72 M.C. Jennings, N.C. Payne and R.J. Puddephatt, Inorg. Chem., 26 (1987) 3776.
73 R.D. Adams and S. Wang, Inorg. Chem., 24 (1985) 4447.
74 R.D. Adams, I.T. Horváth and S. Wang, Inorg. Chem., 25 (1986) 1617.